TRANSIENT PERFORMANCE OF A DUAL-MODE CARRIER-CONTROLLED RELAY SERVOMECHANISM

by

Carrié Dévieux

A thesis submitted to the Faculty of Graduate Studies and Research in partial fulfillment of the requirements for the degree of Master of Engineering.

Department of Electrical Engineering
McGill University
Montreal.

April 1960

SUMMARY

The purpose of this project is to prove theoretically and to demonstrate on a laboratory model that a dual-mode relay servo can be designed which does not have the complexity of the standard type using an ordinary linear amplifier in its linear mode. This is achieved by operating the relays in this region under the control of a linearizing carrier signal.

The experimental investigation is carried out on a model using ordinary servo components such as a two-phase motor, an induction tachogenerator, and associated components which are common to instrument servos. This has the advantage of showing the effect of noise and second-order non-linearities such as backlash and static friction. The performance of the dual-mode carrier-controlled relay servo is judged by its transient response as compared to those of a standard dual-mode type. The comparison is also made with a carrier-controlled linear servo and a standard linear one.

The project involved the design and construction of an electronic switching circuit and of a relay circuit. Improvement of the existing equipment was found necessary. Input and the output signal information of the servo is processed in an analogue computer before being supplied to the switching circuit.

This study leads to the conclusion that the dual-mode carrier-controlled relay servo has a better transient performance than the standard type largely because the switching from one operating mode to the other is smoother. Its static accuracy is also superior in the

presence of backlash. This type of servo will be used at its best in heavy systems like those found in industrial and military applications. In an instrument servo, the improvement obtained is not sufficient to justify the complexity of a switching circuit.

ACKNOWLEDGEMENTS

This project was made possible through Grant No. A-515 from the National Research Council whose help is gratefully acknowledged. The author wishes to express his sincere thanks to Dr. T. J. F. Pavlasek who directed the project and who gave valuable advice in the writing of the thesis.

The help given by Messrs. A. J. Patterson and J. Hargraves of Northern Electric in connection with polarized relays and the assistance of Mr. R. Flegg in the adjustment of some precision components are deeply appreciated. The author wishes also to recall the assistance given by Mrs. M. Neumann of the McGill Engineering Library and by Mr. E. Lavigne of the Library of the Ecole Polytechnique.

A special note of thanks is due to Mrs. H. Brammell who typed the thesis under such difficult circumstances. The author similarly appreciates the work of Messrs. E. Adler and M. L. Blostein who read the proofs and the co-operation of all those who had to stand the 16 db acoustical noise generated by the equipment.

Carrié Dévieux

April 1960
Montreal.

- TABLE OF CONTENTS -

- LIST OF ILLUSTRATIONS -

Chapter I
INTRODUCTION

1.1 Introductory Remarks.

Although automatic control devices have been used for a long time, their systematic study only started some thirty years ago by the work of Minorsky[1] and Hazen[2]. In fact, Minorsky was the first to use the word servomechanism. It is interesting to note that the early works in the field of Feedback Control dealt with non-linear systems of the continuous and discontinuous (relay) types.

The evolution of feedback control has been like that of other branches of science. The early observations and experimentations were followed by the establishment of a general theory; namely, the Theory of Feedback Control explaining the occurence of different phenomena. Predictions about the performance of mechanical systems were possible after solving the differential equations satisfying Newton's Laws. Under certain assumptions, these differential equations could be made linear thus greatly simplifying their solution. This linearization had the enormous advantage of making the study of servomechanisms similar to that of the feedback amplifier[3] where extensive studies of transmission properties and stability had been done by Bode[4] and Nyquist[5].

Despite all the simplifications made possible by the linear approximation, however, it was soon found necessary to return to the study of non-linear systems for two main reasons: first, servomechanisms had to be built much larger than necessary in order to justify the approximations of linearity; secondly, optimum performance could not be obtained with linear systems due to the compromise that had to be made between stability

and accuracy. This gave an impetus to the study and development of non-linear systems . As a consequence of the conditions prevailing at that time, communication was not possible between scientists working on the same problems in different countries. Even today it is felt that there is a lack of organization in research on non-linear systems. The main reason is certainly the very nature of non-linearities which will always escape complete generalization. However, certain classes of non-linearities can be studied in an organized fashion. Actually, it appears that for many workers the design of non-linear systems is more an art than a science. On the other hand, certain theoretical studies of such systems seem to be nothing else than "mathematical exercises...with little regard to practical applications", using the words of Axelby.[6]

The approach towards more organized research in Automatic Control seems to have been by separation of theory and practice. In actual fact, these should develop along parallel lines with the theory leading the way to practical (engineering) applications. This is the idea expressed by Tsien[7] in the preface of his book. He suggests that Feedback Control Theory should be treated as <u>an engineering science</u> (Engineering Cybernetics) much like fluid dynamics. The engineering applications will follow the developments in Engineering Cybernetics. Using the words of Tsien, "...the justification of establishing engineering cybernetics as an engineering science lies in the possibility that looking at things in <u>broad outline</u> and in an <u>organized way</u> often leads to fruitful new avenues of approach to old problems and gives new unexpected vistas!"

The necessity of organized research in non-linear systems has been felt by many workers. Higgins[8] has made an excellent contribution towards that goal by publishing a Bibliography on Non-Linear Control System Theory. A few textbooks treating non-linear systems have been published recently,

the most noteworthy being by Cosgriff[9], Smith[10], and Gille[11].

1.2 Research on Non-Linear Systems.

Purpose: From the study of literature on non-linear servomechanisms, it is noted that the trend of present investigation is to:-

a. Improve stability and transmission performance of systems with inherent non-linearities (saturation, hysteresis, backlash, etc.).

b. Design systems with optimum transient response.

Method: To achieve these two goals, new tools of analysis and synthesis are needed. This is well stated by Smith[12]. The methods of analysis now in use are:-

a. Phase-plane method (method of Poincare)[11]. The phase-plane is a powerful tool of analysis and design. Its usefulness may be questioned, however, for systems of order higher than two, which require a study in N dimensional space. Bogner and Kazda[13] have successfully extended the method to third order systems by applying certain changes of co-ordinates.

b. Describing function method. The describing function method is the extension of the frequency response method for linear systems. It has been used by Kochenburger[14] and others. It allows the prediction of the stability of systems where the non-linearities (amplitude dependent) constitute an independent block from the frequency dependent elements. The describing function method, however, predicts nothing about the transient response.

1.2.1 Design of optimum systems.

A servomechanism is said to have optimum transient performance when it responds to a step input without overshoot and

in a minimum time consistent with the system limitation.

It can be proved easily that it is impossible for a linear system to satisfy both requirements. Work towards optimization of servomechanisms has been carried out on two types of systems:-

a. Continuous systems.

If the damping of a servo is some function of the inverse of the magnitude of the error signal the system can be made to respond faster and without overshoot to step-inputs. McDonald[15] was one of the first to suggest the method. It has been applied by Lewis[16] in the form of a non-linear velocity feedback. Its main drawback is that damping might be excessive for small inputs. Also, the response to a continuous signal like a ramp-input would be impaired. Such a system might be unstable in the presence of noise.

Certain workers, like Kuba and Kazda[17,18] use a more systematic approach. Instead of trying to improve a linear servo, it seems preferable to synthesize the optimum system. After the specification of the desired response as trajectories in a phase-plane or phase-space, a non-linear differential equation is synthesized. The non-linear term is usually the damping factor. Using certain theorems (Liapounoff, Bendixson) predictions can be made about the stability of the system. A model has been designed for step-inputs which, they claim, gives a response time only 11% greater than the ideal on-off servo and which shows definite superiority over a linear one for other kinds of input.

b. Discontinuous system.

Discontinuous systems are those using relays and other switching devices. They have the advantage of simplicity of construction and high power amplification.

A great deal of work has been done in order to improve them. Hazen[2] (1934) was one of the first to study the relay servomechanism and to show under what conditions the amplitude of the steady-state oscillations can be made small. Weiss[19] (1946) used the phase-plane method to study some stabilizing techniques: friction-brake, flip-flop, front-lash, lead stabilization. It is interesting to note that all these techniques correspond to the phase lead stabilization so useful in linear systems. This fact has been clearly noticed by Dutilh[20](1950). His report can be considered to be the first systematic treatment of the relay servomechanism. Dutilh shows how the steady-state oscillations depend on the time delay of the relay, and how the frequency of these oscillations can be increased by reducing the time lags of the servo loop. Since the amplitude of the oscillations decreases with increasing frequency, the steady-state deviations can be made as small as desired.

Dutilh did not carry out the relationship between relay and linear servos any further. It was MacColl's[21](1945) idea to demonstrate that under certain conditions an oscillating servo behaves like a linear servo. The idea has been applied in a Carrier-Controlled Relay Servo by Lozier[22]. Loeb[23,24] generalized the linearizing process to include hereditary effects (hysteresis, backlash).

1.2.2 Programmed servomechanisms.

All the work expressed above was mainly concerned with the stability of relay servos. It can easily be understood, however, that optimum response can be obtained from a system only if such a system is working at its maximum capacity during the reduction of the transient. This calls for a discontinuous controller. When a step-input is applied to a second order electromechanical system, the controller applies a voltage of such polarity to the motor as to make it deliver its forward maximum torque. At a certain time, depending on the error signal and its first derivative, the controller will reverse the voltage producing a braking action. The instant of reversal is calculated by a computer and is such as to reduce the error and its derivatives to zero at the same time, thus preventing any overshoot. When steady state is reached, the computer will command the controller to disconnect the source of power from the motor. It can be proved[25] mathematically than an N^{th} order system requires (N) applications of torque in order to give optimum response. Such servos are given the name of Programmed Servomechanisms.

1.2.3 Dual-mode programmed servos.

The optimization of an N^{th} order servomechanism calls for switching in space of N dimensions. In other words, information about the (N-1) first derivatives of the input ($\dot{\theta}_i$) and output ($\dot{\theta}_o$) positions together with θ_i and θ_o themselves, must be supplied to the computer. The latter is programmed to generate a certain non-linear function of these variables, according to certain parameters of the servo system (inertia J, Damping F, etc.). The sign of this function actuates the controller.

Needless to say, the complexity of any on-off system of an order higher than three will usually prevent its practical realization. A third order servo alone requires a two variable non-linear function generator. Bogner and Kazda[13] have studied such a system, but have made their experimental verification on an analogue computer. In the discussion that follows the paper, Oldenburger shows how noise makes higher order systems impractical. According to Silva[26,27], in an N^{th} order on-off servo the first two applications of torque last much longer than the (n-2) remaining. Imperfections in relay and controller suggest that for all practical purposes an ideal N^{th} order (Type I) system can be approximated by a second-order one (Type II) on the condition that proportional control is provided for a certain range of errors in order to take care of the stored energy. This is what is called a Dual-Mode Programmed Servo. The idea of dual-mode control had already been suggested by McDonald[15] in order to improve the performance of the non-off servo for continuous inputs (ramp, etc.). Its main disadvantage is its complexity.

1.3 Object of the Thesis.

The object of this thesis is the experimental verification of the performance of a dual-mode programmed servo not requiring the use of a standard linear power amplifier. Using the ideas of MacColl, Loeb, Lozier, an oscillating relay system is used in the linear mode. Following Dutilh, the external carrier is replaced by the self-oscillations of the relay system. Transient responses of this carrier-controlled dual-mode servo are compared to those of an ordinary dual-mode servo, to those of an oscillating relay servo and also to those of a "linear" servo exhibiting saturation in its amplifiers.

The reasons for carrying this investigation are:-

a. Such a system has the advantage of simplicity of construction since the same relay system is used in both modes of operation.

b. Relays are the most efficient power amplifiers. For heavy servos like gun tracking systems, the relays can be replaced by clutches[28], eliminating the amplidyne and the Ward-Leonard System.

c. The transition from one mode to the other can be made faster and smoother.

d. As far as is known, the study of such a system has not appeared in the literature.

1.3.1 Equipment.

The tests are made on a position servo powered by a two-phase, 60 cycle motor. This equipment has been built by C. F. Caswell[29]. For the investigation of the dual-mode operation an electronic switching circuit had to be built to replace the existing purely mechanical switching circuit. Results are recorded on an oscilloscope and on a Sanborn recorder.

Chapter II

STUDY AND DESIGN OF THE DUAL-MODE PROGRAMMED SERVO

ON-OFF MODE

2.1 Introduction.

An optimum position servomechanism is one which responds to a step-input without overshoot and in a minimum time consistent with the system limitations. Before trying to find conditions under which a servomechanism can be optimized, it will be necessary to review briefly the linear servomechanism. An analysis of the dual-mode servo, and the design of the model, will follow.

2.1.1 Linear servomechanism.

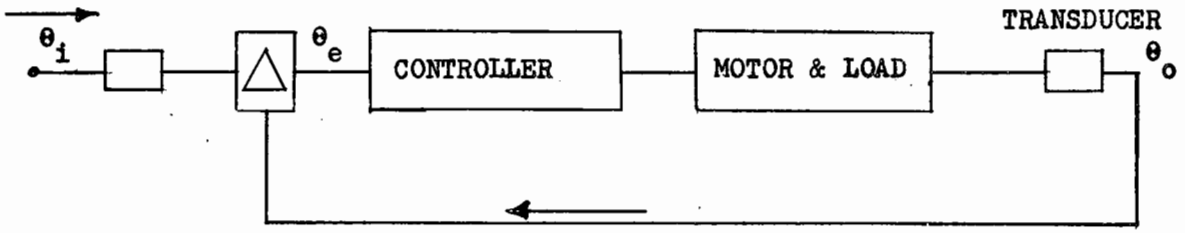

Figure 2.1 Simple Position Servomechanism

θ_i = Input position angle
θ_o = Output position angle
θ_e = $\theta_i - \theta_o$ = Error or Deviation
$\dot{\theta}$ = $d\theta/dt$ = 1st derivative of θ
T = Motor output torque
K = T/θ_e = Gain of linear controller
J = Motor and load inertia
F = Viscous damping in the system.

In the general position servomechanism (Fig. 2.1), the feedback loop tends to correct for any difference θ_e between the

input position θ_i and the output position θ_o. The controller makes the motor deliver a correction torque $T = f(\theta_i, \theta_o)$. For a second-order system

$$J\ddot{\theta}_o + F\dot{\theta}_o = T \qquad (2.1.1)$$

In a linear servomechanism, the controller is a linear power amplifier of gain K.

$$J\ddot{\theta}_o + F\dot{\theta}_o = T = K(\theta_i - \theta_o) = K\theta_e \qquad (2.1.2)$$

In the case of a relay servo, the controller is a relay and the correction torque is

$$T = T_{max}\ \mathrm{sgn}(\theta_i - \theta_o) \qquad (2.1.3)$$

$$J\ddot{\theta}_o + F\dot{\theta}_o = T_{max}\ \mathrm{sgn}(\theta_i - \theta_o) \qquad (2.1.4)$$

2.1.2 Effect of saturation.

In an ideal linear servomechanism satisfying equation (2.1.2), response (rise) time depends only on the parameters J, F, K and is completely independent of the magnitude of the step-input. Any physical system, however, will have a maximum value (T_{max}) of output torque. The differential equation describing the system for values of (θ_e) producing saturation will be (2.1.4). The analysis of a "linear" servomechanism exhibiting saturation must then be made "piecewise". In the saturation region, response time will increase with the magnitude of the step input... The relay servo can be considered as being the limiting case of a linear saturated type where the gain (K) is infinite.

2.1.3 Conditions for optimum response.

Bellman, Glicksberg and Gross[24] have given two mathematical

theorems showing under what conditions an N^{th} order system can have a minimum response time when the forcing term (T) must satisfy certain constraints. These theorems are quite general. They can be translated into the engineer's language to constitute the following theorem.

2.1.4 Theorem.

The response time of a system described by an N^{th} order linear differential equation whose characteristic roots all have negative real parts, and whose forcing term (f) has to satisfy the constraint $|f| \leq 1$, is a minimum, for a step input, if $|f| = 1$ and if f changes sign at most (N-1) times.

This shows that an optimum servomechanism must be of a discontinuous (relay) type and necessitates the use of an "intelligence" (computer) to operate the (N-1) reversals of correction torques at the right time. A substantial portion of the present thesis consists of the design of such a switching circuit. Before going to the description of such a circuit it will be necessary to study the operation of an ideal on-off servo in some detail, and in particular, investigate its steady-state performance more carefully.

2.1.5 Phase-plane (space) techniques.

A system whose differential equation is of the N^{th} order is said to have N degrees of freedom because its physical state at any time (t) is described by N different variables. In an N^{th} order servomechanism these variables are θ_o and its (N-1) derivatives. These time dependent variables are called generalized (dynamic) co-ordinates because they allow the description of its performance in terms of energy relations which are the fundamental

entities in a dynamic system. The description of an N^{th} order system by its generalized co-ordinates is said to take place in the phase-space of N dimensions.

When the differential equation is linear, it is much easier to find the analytic solution of θ_o as a function of time, given the initial conditions. The usefulness of the phase-space method is fully appreciated only when the equation is non-linear, because the trajectories can be constructed graphically. Time of response and stability can be studied from these graphs.

2.1.6 Time constants of servomechanisms.

Most linear servomechanisms can be described accurately enough by the second-order differential equation (2.1.2)

$$J\ddot{\theta}_o + F\dot{\theta}_o = K(\theta_i - \theta_o) \qquad (2.1.2)$$

The left hand side represents the only frequency dependent terms of this equation. It represents the characteristics of the motor and load combination. By Laplace transformation, the open-loop transfer function is

$$\frac{\theta_o}{\theta_e} = G(P) = \frac{K}{FP(\frac{J}{F}P+1)} = \frac{K}{FP(PT_m+1)} \qquad (2.1.5)$$

where $T_m = \frac{J}{F}$, is the motor time constant.

If the other time constants of the servo loop (field windings, amplifier, etc.) cannot be neglected, the transfer function becomes

$$G(P) = \frac{K'}{P(PT_m+1)(PT_1+1)(PT_2+1)\ldots(\quad)\ldots} \qquad (2.1.6)$$

The time constants ($T_1, T_2 \ldots$) account for the "hunting" of so called second-order systems which, according to the theory,

should never oscillate. However, they are often small enough to justify the second-order approximation.

Bogner and Kazda[13] have studied analytically and experimentally the switching criteria of the third-order on-off servo on an analogue computer. The mathematics are already very complex. For the purpose of illustrating the operation of an on-off servo a theoretical study of a second-order system will be sufficient. Trajectories in the phase-plane will be drawn for the case where there is no viscous damping and compared to those of a system with friction damping.

2.1.7 Phase-plane trajectories.

The phase-plane portrait of a second-order servo is a plot of output velocity ($\dot{\theta}_o$) against output position θ_o. It is a plot of the function $\dot{\theta}_o = f(\theta_o)$ or $\theta_o = G(\dot{\theta}_o)$. These curves can be drawn without knowing the analytic solution (Gille[11], Cosgriff[9]) by making certain changes of variable in the differential equation. This method had been suggested by Poincaré.

Let the second order differential equation be

$$\frac{d^2x}{dt^2} = f(x, \frac{dx}{dt}) \qquad (2.1.7)$$

Let $y = \frac{dx}{dt}$ (2.1.8)

Then equation (2.1.7) is equivalent to the system

$$\frac{dx}{dt} = y \qquad (2.1.8)$$

$$\frac{dy}{dt} = f(x,y) \qquad (2.1.9)$$

Then $$\frac{dy}{dx} = \frac{f(x,y)}{y} \qquad (2.1.10)$$

For the second order linear servomechanism

$$J\ddot{\theta}_o + F\dot{\theta}_o = K(\theta_i - \theta_o) \qquad (2.1.2)$$

$$\frac{d(\dot{\theta}_o)}{dt} = \ddot{\theta}_o = \frac{K(\theta_i - \theta_o) - F\dot{\theta}_o}{J} \qquad (2.1.11)$$

$$\dot{\theta}_o = \frac{d(\theta_o)}{dt} \qquad (2.1.12)$$

$$\frac{d(\dot{\theta}_o)}{d(\theta_o)} = \frac{K(\theta_i - \theta_o) - F\dot{\theta}_o}{J\dot{\theta}_o} \qquad (2.1.13)$$

The integration of 2.1.13 might prove to be very difficult except for special cases like the one when $F = 0$, $\theta_i = c$, the solution being an ellipse described by

$$A\theta_o^2 + B\dot{\theta}_o^2 = C_1 \qquad (2.1.14)$$

The advantage of the phase plane technique lies in the fact that transient responses ($\theta_i = c$) can be drawn graphically by the method of isoclines. The isoclines are curves defined by

$$\frac{dy}{dx} = \frac{f(x,y)}{y} = m.$$

For linear systems, they are straight lines passing through the origin if $\theta_i = 0$. The slope of the phase plane trajectory at the point of intersection with the isocline is (m). Knowing the initial conditions $\dot{\theta}_{oi}$ and θ_{oi}, a trajectory can then be sketched to satisfy the slope (m) at the intersection with the isocline (Figure 2.2)

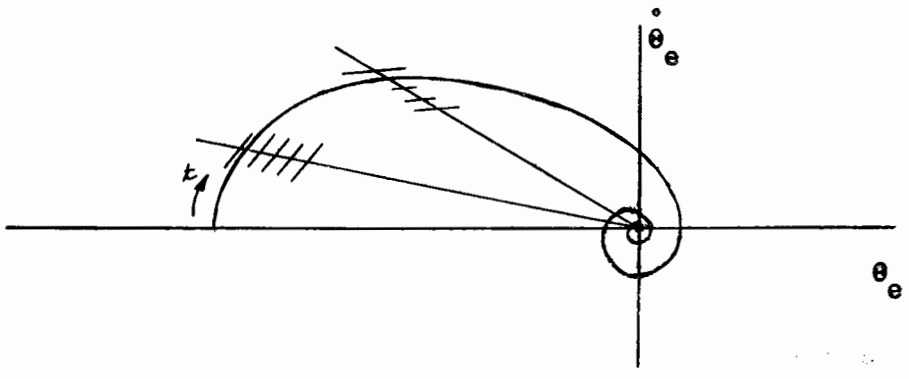

Fig. 2.2 Damped transient response of Eq. 2.1.2

It is found more convenient to plot the transient response in terms of error (θ_e) and error velocity ($\dot{\theta}_e$) as in Figure 2.2 because for a stable system, those two quantities become zero after a certain time.

STABILITY. Strictly speaking there is stability only if all trajectories end up at the origin. There is instability when the trajectories move away from the origin. Damage might then occur to the system unless those trajectories end up on a closed boundary named the limit cycle. This boundary is determined by the saturations present. A limit-cycle oscillation is then strictly a non-linear phenomenon. Its amplitude is independent of the initial conditions of position and velocity. Under certain conditions a system whose steady state is a limit-cycle oscillation can be considered to be stable. It must be noted that even if all trajectories seem to end up at the origin, the steady state might in fact be a limit cycle which would be apparent if the scale were enlarged.

RESPONSE TIME. The response time is the time taken to reduce the transient error and velocity within certain limits. If no limit is set, the response time of a linear system is found to be theoretically infinite. In the case of a linear system, the response (rise) time is usually taken as the time required to reduce the transient error from 90% to 10% of its initial value.

The time interval between any two points on a trajectory can be found from the integral

$$t_{12} = \int_{x_1}^{x_2} \frac{dx}{y} = \int_{\theta_{01}}^{\theta_{02}} \frac{d\theta_o}{\dot{\theta}_o} \qquad (2.1.15)$$

The time interval is then equal to the area under the curve $(\frac{1}{y})$ limited by x_1 and x_2.

2.2 Analysis of a "Second-Order" Dual-Mode Servo.

2.2.1 Phase-plane trajectories.

According to Theorem (2.1.4), optimum response is achieved for a second-order system by two applications of maximum torque. Its transient response will therefore be represented by two trajectories in the phase-plane (Figure 2.3) each of which is determined by a linear differential equation with a constant forcing

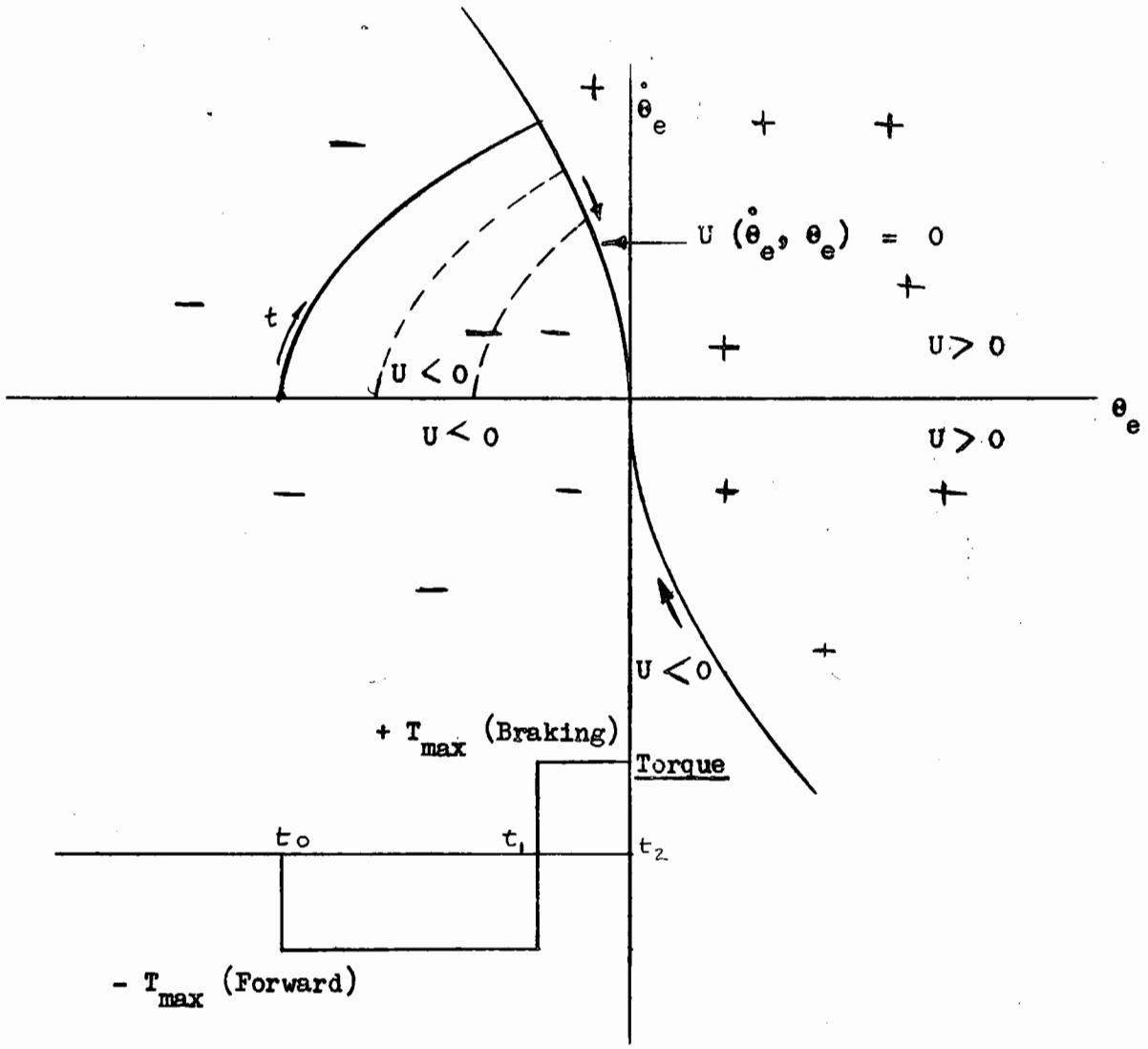

Fig. 2.3 Phase-plane trajectories of a second-order on-off servo and torque applications.

term. At equilibrium, when the error (θ_e) and the first derivative of the error ($\dot{\theta}_e$) both become zero, the torque is also reduced to zero.

If the phase-plane portrait is drawn for the error variables, all trajectories will end up at the origin for a step input. It can be proved easily that only one trajectory can pass through any point in the phase plane. This means that the deceleration trajectory is unique when the input is a step. The function $U(\dot{\theta}_e, \theta_e) = 0$, which describes that curve, is called the switching function of the on-off servo.

2.2.2 Calculation of trajectories.

The trajectories are calculated from equation (2.1.1) by making the forcing term the constant $\delta \cdot T_{max}$.

$$\boxed{J\ddot{\theta}_o + F\dot{\theta}_o = \delta T_{max}} \qquad (2.2.1)$$

$$\delta = \text{sgn } U(\dot{\theta}_e, \theta_e) \qquad (2.2.2)$$

δ = switching coefficient

Acceleration trajectory.

$\delta \geq 0$ for a positive step input ($\theta_i = +c$)

$$J\ddot{\theta}_o + F\dot{\theta}_o = +T_{max} \qquad (2.2.3)$$

$$\frac{d\dot{\theta}_o}{d\theta_o} = \frac{T - F\dot{\theta}_o}{J\dot{\theta}_o} \qquad (2.2.4)$$

$$\theta_o \Big|_{\theta_{oi}}^{\theta_{of}} = -\frac{J}{F}\left\{\dot{\theta}_o + \frac{T}{F}\ln\left|T - F\dot{\theta}_o\right|\right\}_{\dot{\theta}_{oi}}^{\dot{\theta}_{of}} \qquad (2.2.5)$$

The maximum output velocity is

$$\dot{\theta}_{omax} = \frac{T}{F} \tag{2.2.6}$$

Initial conditions

$$\left.\begin{aligned} \theta_i &= +c & \dot{\theta}_i &= 0 \\ \Delta_{oi} &= 0 & \dot{\theta}_{oi} &= 0 \end{aligned}\right\} \tag{2.2.7}$$

Equation (2.2.5) can be written for the error variables making the following substitutions

$$\left.\begin{aligned} \theta_e &= \theta_i - \theta_o \\ \Delta\theta_e &= \Delta\theta_i - \Delta\theta_o \\ \dot{\theta}_e &= \dot{\theta}_i - \dot{\theta}_o \end{aligned}\right\} \tag{2.2.8}$$

$$\boxed{\theta_{ef} = C + \frac{J}{F}\left(-\dot{\theta}_{ef} + \frac{T}{J}\ln\left|1 + \frac{F}{T}(\dot{\theta}_{ef})\right|\right)} \tag{2.2.9}$$

This is the acceleration trajectory for a <u>positive step input</u> $\theta_i = +c$. It occupies the 4th quadrant.

For negative step inputs the curve occupies the 2nd quadrant and is symmetrical to the previous one.

<u>Deceleration trajectory</u>.

The deceleration trajectory for a positive step input is found easily from (2.2.5) by replacing +T by -T and by substituting

$$\theta_{of} = c$$

$$\dot{\theta}_{of} = 0$$

$$C - \theta_o = -\frac{J}{F}\left\{-\dot{\theta}_o + \frac{T}{F}\ln\left|1 + \frac{F}{T}\dot{\theta}_o\right|\right\} \tag{2.2.10}$$

$$\boxed{\theta_e = -\frac{J}{F}\left\{\dot{\theta}_e + \frac{T}{F}\ln\left|1 - \frac{F}{T}\theta_e\right|\right\}} \tag{2.2.11}$$

For a negative step input, equation (2.2.11) still holds since T, $\dot{\theta}_e$ and θ_e reverse signs. The two curves lie in the 4th and 2nd quadrant respectively and are symmetrical with respect to the origin.

The switching function is

$$\boxed{U(\theta_e,\dot{\theta}_e) = \theta_e + \frac{J}{F}\left\{\dot{\theta}_e + \frac{T}{F}\ell n\left|1 - \frac{F}{T}\dot{\theta}_e\right|\right\}} \qquad (2.2.12)$$

Note: when $\theta_i > 0$, $\theta_e > 0$ and $\dot{\theta}_e < 0$

The complete switching curve $U(\theta_e,\dot{\theta}_e)$ divides the phase plane in two regions as shown in Figure 2.3. $U(\theta_e,\dot{\theta}_e)$ is positive above the curve and negative below.

2.2.3 Behaviour of the on-off system around the origin ($\theta_e = \dot{\theta}_e = 0$).

Referring to Figure 2.3, it is seen that for an ideal on-off system the torque is reduced to zero when both θ_e and $\dot{\theta}_e$ are zero. This last statement is only a limiting case and has no meaning for a physical system. A more realistic statement would be:-

The servo reaches equilibrium when both θ_e and $\dot{\theta}_e$ satisfy the relation

$$|\theta_e| < \varepsilon_1 \qquad (2.2.13)$$

$$|\dot{\theta}_e| < \varepsilon_2 \qquad (2.2.14)$$

ε_1 and ε_2 depend on the precision of the physical components, and on the amplitude of the noise.

2.2.4 Dual-mode system.

In the region where (2.2.13) and (2.2.14) are satisfied, the system is force-free and any stored energy is absorbed by the viscous friction. This shows that any physical on-off servo

is in fact of the dual-mode type.

In some simple industrial systems, very high damping is provided in the second-mode region to insure stability. In more accurate servo systems, a standard linear controller is provided in the second mode. This is the type being investigated in this thesis with the difference that the linear control is achieved by a superimposed carrier as explained later. Such a combination has the advantage of retaining the original simplicity of the on-off method.

2.2.5 Detailed analysis of the steady state of the on-off system with dead-zone.

The steady state of an on-off servo is a limit-cycle oscillation in the dead-zone. In that region, it behaves like an ordinary relay type with error and error-rate control.

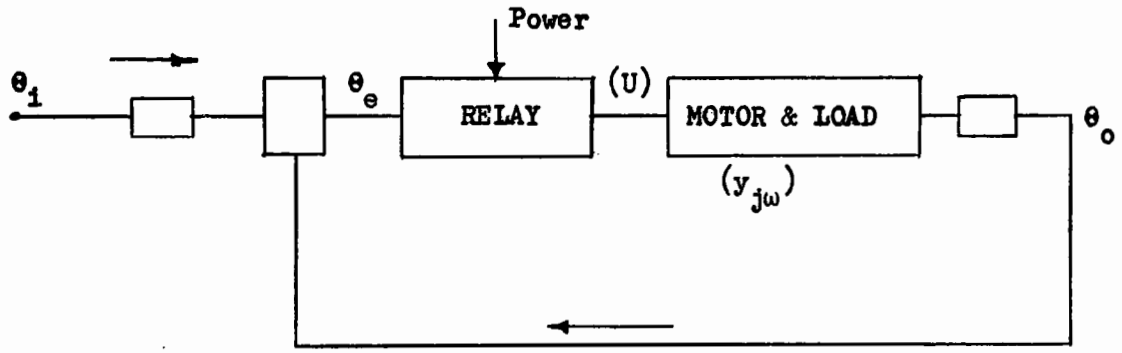

Fig. 2.4 Simple Relay Servo

Where θ_e = error signal; u = relay output voltage

A simple relay servo is represented in Figure 2.4. When the relay is oscillating at the frequency (ω_o), its output (U) is a square wave of amplitude (U_o). The filtering produced by the motor and load combination is usually sufficient to make all

harmonics negligible. The output (θ_o) can be considered to be a sine wave of frequency (ω_o).

As for linear systems, the relay servo will keep oscillating only if $\frac{\bar{\theta}_o}{\bar{\theta}_e} = -1$. This can be broken down into the two requirements

a. Loop gain: $$A = \frac{|\theta_o|}{|\theta_e|} = 1 \qquad (2.2.15)$$

b. Total loop phase shift: $$\phi_{(\omega_o)} = \pi \qquad (2.2.16)$$

Relay threshold and time delay.

If the relay has a threshold ε_o, it will be operated only by signals θ_e larger than ε_o. Also, the amplitude of the fundamental frequency in the output (U) will vary with the amplitude of (θ_e). The threshold therefore affects the loop gain (A). If it is made large enough, no oscillation will take place. This is one means of stabilization that has been used in the past at the expense of the accuracy of the servo. Mathematically, the condition for the non-existence of the oscillation is

$$\boxed{\varepsilon_o > \frac{1}{2}\frac{4}{\pi} U_o \left| Y_{(j\omega_o)} \right|} \qquad (2.2.17)$$

where $Y_{(j\omega)}$ is the transfer function of the motor and load combination.

If U_o is the square wave amplitude, the amplitude of the fundamental in the absence of threshold is

$$B_1 = \frac{4}{\pi} U_o \qquad (2.2.18)$$

If there is a threshold (ε_o), the amplitude is

$$B_2 = B_1 \sin \alpha = \frac{4}{\pi} U_o \sin \alpha \qquad (2.2.19)$$

where $\cos \alpha = \frac{\varepsilon_o}{\theta_e}$ (2.2.20)

Time delay.

If there is a time delay (τ), the frequency of oscillations will be (f_o) such that

$$\phi_{(\omega_o)} + \omega_o T = \pi \tag{2.2.21}$$

$$\omega_o = \frac{\pi - \phi_{(\omega_o)}}{T} \tag{2.2.22}$$

$$\omega_o = 2\pi f_o$$

Since the amplitude (θ_o) decreases with an increase in frequency (ω_o), improving the accuracy of the relay servo requires a reduction of the lag phase shift (ϕ_{ω_o}). In other words, some phase lead will have to be provided in the loop.

On-off systems.

Considering again the on-off servo, it is seen that the steady-state is a limit-cycle oscillation in the dead-zone. An ideal on-off servo would oscillate at infinite frequency and zero amplitude. For a physical system, both frequency and amplitude are finite. These oscillations are not a disadvantage, however, because as has been proven by MacColl, Loeb and others, an oscillating servo behaves like a linear one for small inputs. By proper adjustment of the frequency (f_o) of the oscillations it is then possible for the on-off servo to follow continuous inputs without the use of a standard linear controller in the dead-zone. The oscillating servo will be described in Chapter III.

2.2.6 Switching function for on-off servo with ramp-input.

Since the on-off servo is of a discontinuous type, its performance will be degraded if it has to respond to a continuous

input, unless some linear controller is provided in the dead-zone. The on-off mode will operate only if a transient is initiated; for example, when the input is a step-plus-ramp. The optimum system will be the one which will reduce the transient and transfer control to the linear mode in the minimum time. According to this definition, it is clear that the switching function must incorporate some information about the continuous function. This is entering the field of adaptive servomechanisms. The added complication of the controller is not justified, however, because of inevitable inaccuracies in the components and because the so-called second-order systems are often approximations of third-order systems. The dual-mode control gives theoretically a quasi-optimum response, but for all practical purposes it can be considered to give the optimum response.

The complexity which would be introduced in the switching circuit for continuous inputs can be easily shown as follows.

The fundamental equation (2.2.1) will be rewritten in terms of the variables (θ_e).

$$J\ddot{\theta}_o + F\dot{\theta}_o = \delta T \qquad (2.2.1)$$

Susbstituting

$$\theta_o = \theta_i - \theta_e$$

$$J\ddot{\theta}_i - J\ddot{\theta}_e + F\dot{\theta}_i - F\dot{\theta}_e = \delta T$$

$$+J\ddot{\theta}_e + F\dot{\theta}_e = -\delta T + J\ddot{\theta}_i + F\dot{\theta}_i \qquad (2.2.23)$$

In the case where the input is a combination of a positive step and some continuous function of time, the deceleration trajectory

or the switching function is the solution $U(\theta_e, \dot{\theta}_e, \dot{\theta}_i, \ddot{\theta}_i)$ of (2.2.23) where

$$\underline{\delta < 0}$$

For a step-plus-ramp input, the equation becomes

$$J\ddot{\theta}_e + F\dot{\theta}_e = +T + F\omega_1$$

If $\underline{\theta_i = C_o + \omega_1 t}$

The switching function is then

$$\boxed{U_{(\theta_e, \dot{\theta}_e, \dot{\theta}_i)} = \theta_e + \frac{J}{F}\left\{\dot{\theta}_e + \frac{T+F\omega_1}{F} \ell n \left| 1 - \frac{T}{T+F\omega_1}\dot{\theta}_e \right|\right\}} \quad (2.2.24)$$

Note: From Equation (2.2.23) it can be easily seen that if a switching function is designed for a certain class of inputs, (step-plus-ramp), it will handle also a lower class of inputs (step-plus) as long as the inputs can be described by the polynomial $a_0 + a_1 t + a_2 t^2 \ldots$ (Neiswander and MacNeal)[30].

If there is no friction (F) in the system, the switching function for a step and for a step-plus-ramp input will be exactly the same.

Remembering that (δ) is a switching coefficient which assumes values -1, +1 and zero successively, it can be deduced from Equation (2.2.23) that the steady state of the servo will be a limit-cycle oscillation for a continuous input since the forcing function will never be zero.

2.2.7 Summary of the factors making dual-mode control a necessity.

It has been shown above that dual-mode control is required for the following reasons:-

a. To take care of the errors made in approximating a third-

order servo by a second-order one. The second time lag is usually due to the inductance of the field winding of the motor. As a matter of fact, the model used in the present investigation has two time lags of about 2.3 sec. and 50 milliseconds.

b. To allow the system to follow continuous inputs.

c. To take care of switching inaccuracies.

2.2.8 Analysis of some significant trajectories.

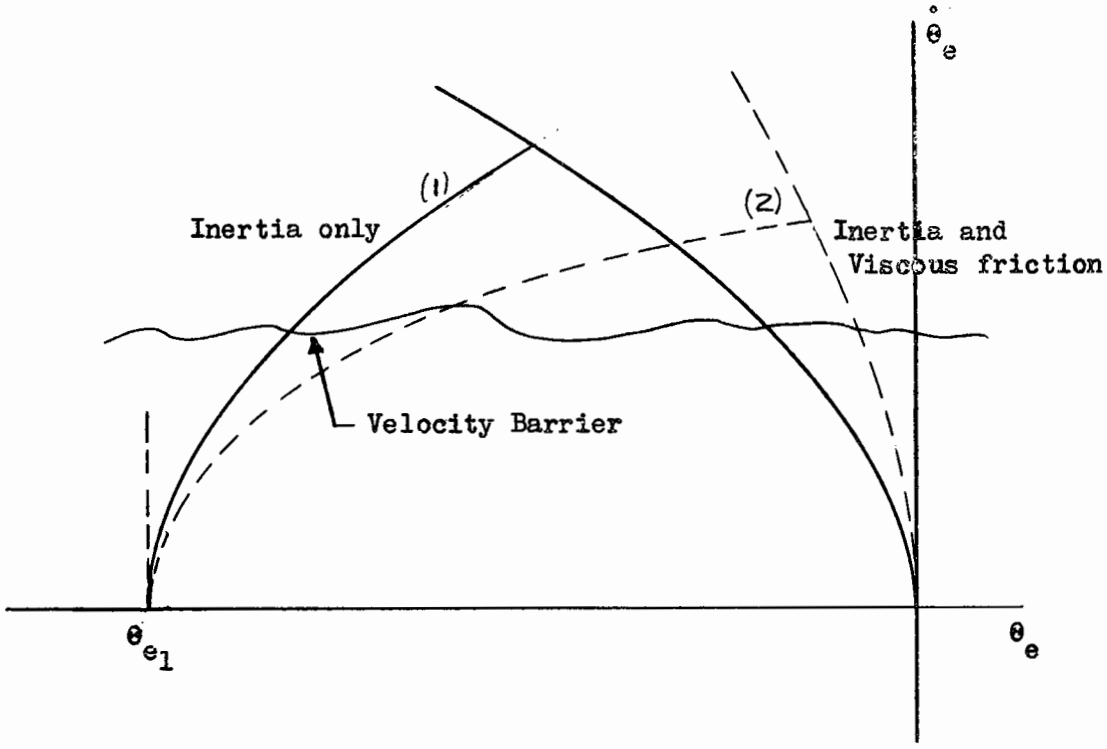

Fig. 2.5 Phase-plane trajectories of second-order system.

In Figure 2.5 are shown the phase-plane trajectories for two second-order systems, one having inertia only and the other, inertia and viscous friction. For the first one, the trajectories are parabolic and consequently they constitute a symmetrical figure. For the second one the acceleration and the deceleration trajectories are not the same. The deceleration trajectory is steeper because the viscous friction helps the braking. The

viscous friction also limits the velocity to the maximum value of T/F. See Equations (2.2.6), (2.2.9) and (2.2.11).

The larger the area enclosed by the trajectories, the smaller will be the response time. Velocity saturation will therefore increase the response time. For the same reason, viscous friction tends to reduce the speed of response. In a second-order system, the trajectories intersect at the point of torque reversal with a sharp corner, and they make a 90^{o} angle with the θ_e axis, as can be deduced from (2.2.4).

A.C. Servomechanisms.

In the servo model used in this investigation, the motor is a 2-phase Diehl induction motor with high rotor resistance. The output torque of the motor with a constant applied voltage is

$$T = T_{max} - F\dot{\theta}_o \qquad (2.2.25)$$

If no viscous friction is present in the system, Equation (2.2.3) becomes

$$J\ddot{\theta}_o = T_{max} - F\dot{\theta}_o \qquad (2.2.26)$$

$$J\ddot{\theta}_o + F\dot{\theta}_o = T_{max}$$

The torque speed characteristics of the motor furnish some friction damping to the system and the trajectories will be like (2) in Figure 2.5.

The disadvantage of excessive damping is that the deceleration trajectory becomes too steep making accurate switching difficult.

Effect of torque-rate saturation and relay time delay.

If the time constant (T_2) of the control field of the

motor is not negligible, the system becomes a third-order one and is said to have torque-rate saturation. A step of voltage applied to the field produces an exponentially rising torque. The effect is to produce a rounded corner at the point of switching (Figure 2.6). Also, the slope of the acceleration trajectory as given by (2.2.4) is finite at time $t = 0^{+}$. This can be shown by replacing the forcing term (T_{max}) by $T_{max}(1-e^{-t/t_2})$.

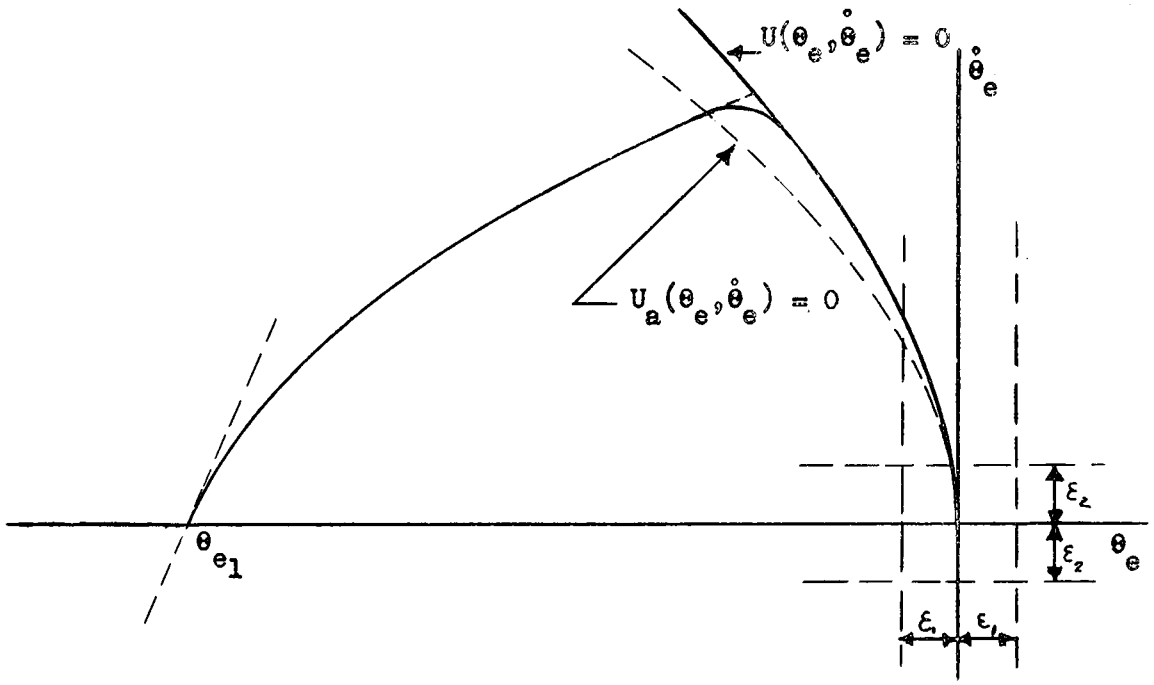

Fig. 2.6 Effect of torque-rate saturation

Torque-rate saturation disturbs the optimum operation of the system. Time delays in the relays also have this effect. This can be corrected by advancing the switching point in applying the correction to the factor $\frac{T}{F}$ in Equation (2.2.12). This is done quite easily. If the time constant T_2 of the motor and the time delay (Υ) of the relays are small compared to the time constant of the motor, the correction applied by advancing the switching curve will be quite sufficient.

Effects of switching inaccuracies are absorbed by the linear controller of the dual-mode control system. In practice, the region of linear control is for the range of error values given by $|\theta_e| < \varepsilon_1$.

2.3 Design of the Dual-Mode Carrier-Controlled Servo.

2.3.1 Design of the controller of the dual-mode servo model.

The model dual-mode servo makes use of the components of the standard linear servo described in Chapter III. Its design will, therefore, be limited to the controller. The block diagram of a dual-mode servomechanism is shown in Figure 2.7.

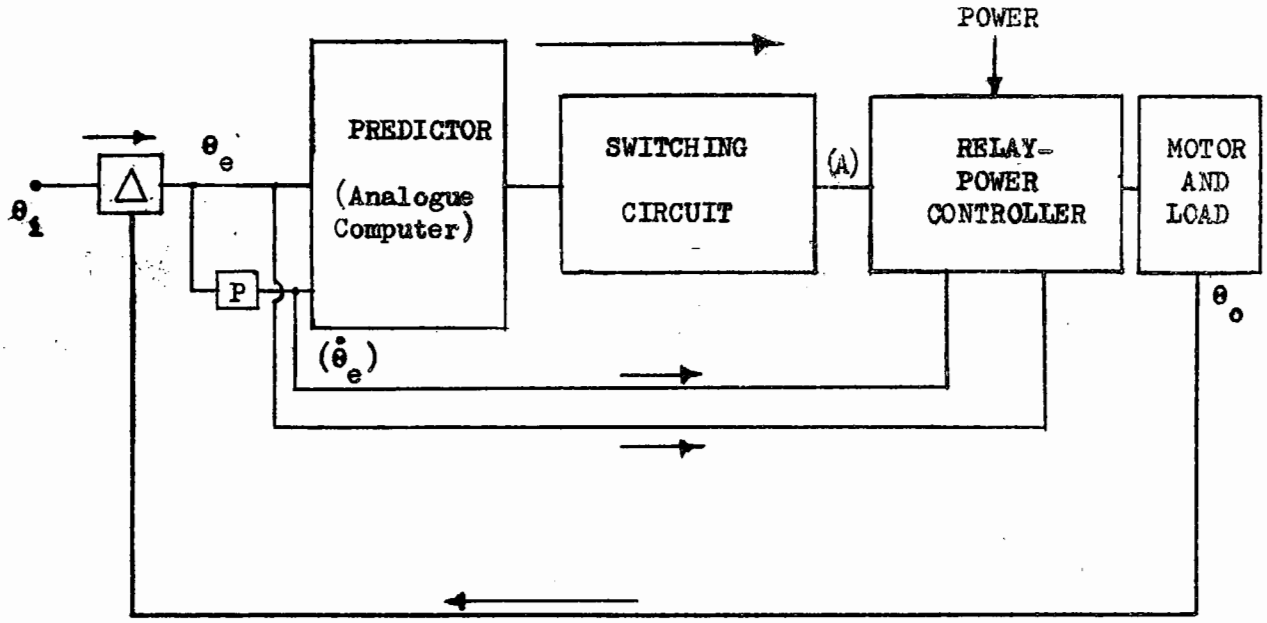

Fig. 2.7 Dual-mode servomechanism

The predictor is an analogue computer programmed to generate the function $U(\theta_e, \dot{\theta}_e)$. The sign of that function is detected by the switching circuit which commands the on-off controller and actuates the linear mode in the "dead-zone".

The contribution of the present investigation consists of combining both controllers into a single unit. For purposes of comparison, the servo can operate as a dual-mode oscillating, dual-mode standard, carrier-controlled (or oscillating) and ordinary linear.

Caswell has computed the switching function $U(\theta_e, \dot{\theta}_e)$ using the system parameters and has also designed a switching circuit using mechanical (relays) components. The difficulties experienced with that circuit prompted the design of the present one which is completely electronic. In this fashion, all logic operations are done at low-power levels. The final stage of power switching is done by relays for both on-off and linear controlling action. This arrangement allows the use of lighter relays with fewer contacts. Time delays and other relay errors are reduced to a minimum. The reversal time delay of the relays used is less than 10 milliseconds as compared to 40 milliseconds for the completely mechanical circuits. The description of the complete controller will start with the power section.

2.3.2 Relay power controller.

The servo uses a two-phase induction motor. As shown in Figure 2.8, the purpose of the relay system is to control the voltage applied to the motor winding. The output torque changes sign if the phase of the 60-cycle control voltage (V_c) is shifted by 180^o. It is proportional to the amplitude of the applied voltage.

In a dual-mode servo, using a standard linear amplifier in its linear mode, the switching relay circuit has to perform

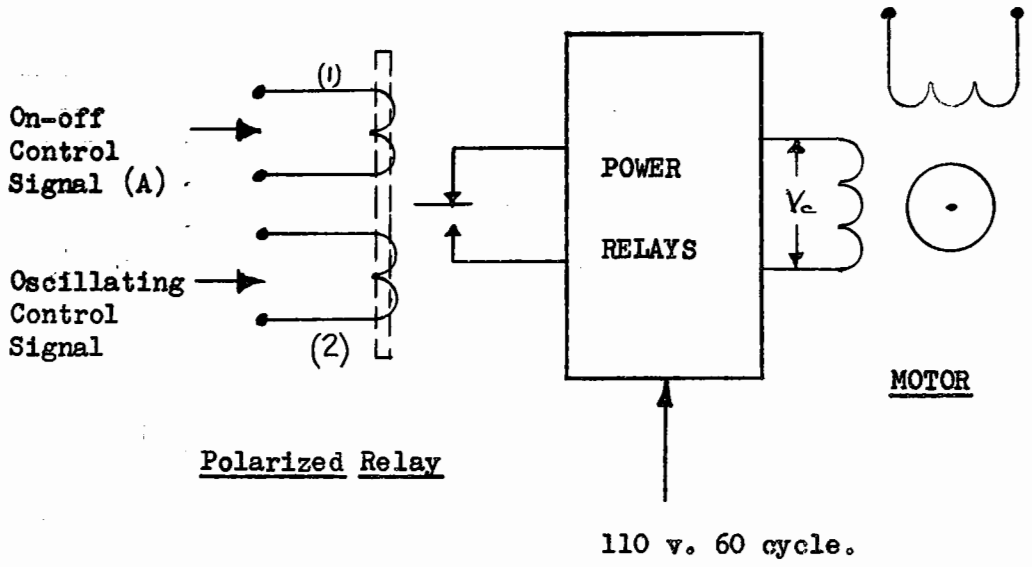

Fig. 2.8 Relay power controller

the operations shown in Figure 2.3 and Figure 2.6; namely,

a. apply line voltage $+\overline{V}_c$ at time t_o.

b. reverse line voltage at t_1.

c. disconnect the line voltage and connect the linear power amplifier to the control winding at t_2.

The relays must then have <u>three positions</u> in the standard dual-mode system.

In the carrier controlled dual-mode servo operation (c) is eliminated, because as explained in Chapter III, linear control is achieved by periodic switching of the voltage V_c. The only difference between the two regions is <u>a change in the mode of switching</u> from controlled to periodic. A homogeneous system has thus been obtained.

The fact that the line voltage does not have to be disconnected from the control winding at any time allows the use

of two-position relays. However, in order to protect the equipment in case the oscillating control voltage vanishes accidentally, a three-position relay system is used. It takes the form of a set of two double-pole, double-throw (DPDT) relays. This arrangement is also necessary in order to perform the tests on a standard dual-mode servo. The complete circuit diagram of the relay power controller is given in Appendix A-1.

Control of the switching modes.

The heart of the power controller is a very sensitive low power polarized relay with two control coils (R = 1000 ohms). The relay is a Northern Electric Type 280E-G, operating at 0.3 ma in about 1 millisecond. The contact arrangement is single-pole double-throw (SPDT). The polarized relay controls the high power relays (Figure 2.8).

Coil No. 1 is controlled by the command signal from the switching circuit which appears as a d.c. voltage having the values +A, -A or zero. Coil No. 2 receives the oscillating control signal which is a low frequency oscillation ($f \simeq 5$ c/sec.) of peak-to-peak amplitude (E) added to the d.c error signal. The voltages are chosen such that $|A| \gg E$. The command voltage A then has complete control of the operations. Oscillating control is resumed as soon as (A) becomes zero. As a consequence the passing from one mode of switching to the other is made quite "smooth". For the operation of the servo as a standard dual-mode one, it has been found necessary to use a second polarized relay which is operated by the gate voltage of the switching circuit. This is shown in Appendix A-1.

2.3.3 Study of the switching circuit logic.

The operations to be performed by the switching circuit can be deduced easily from Figures 2.3 and 2.6. Following the suggestions of McDonald and others, the range of the linear mode is defined by

$$|\theta_e| < \varepsilon_1 \qquad (2.2.13)$$

For an ideal on-off servo, the function of the switching circuit is to give a d.c. output voltage (A) such that

$$(A) = A \operatorname{sgn} U(\theta_e, \dot{\theta}_e) \qquad (2.3.1)$$

$$(A) = 0, \text{ when } \theta_e = \dot{\theta}_e = 0$$

$$\text{or} \quad U \equiv 0$$

$$U(\theta_e, \dot{\theta}_e) = M\theta_e + f(\dot{\theta}_e) \qquad (2.2.12)$$

The fact that $U(\theta_e, \dot{\theta}_e) = 0$ on the deceleration trajectory is a cause of instability for a practical system where noise and other errors are unavoidable. This is the reason why the switching circuit must have a built-in memory which will prevent any subsequent torque reversal until the transient has completely disappeared. The memory takes the form of a flip-flop operated by a Schmitt trigger to which is fed the switching function $U(\theta_e, \dot{\theta}_e)$. The fact that the output (A) is a d.c. voltage necessitates the design of two channels, one for the positive and one for the negative polarity.

The second condition of Equation (2.3.1) requires a gate circuit controlled by either $(\dot{\theta}_e)$ or (θ_e). However, as shown earlier, any practical on-off servo is of the dual-mode type and

the dead-zone is the area around the origin shown in Figure 2.6 and defined by

$$\left| \theta_e \right| < \varepsilon_1 \qquad (2.2.13)$$

$$\left| \dot{\theta}_e \right| < \varepsilon_2 \qquad (2.2.14)$$

In practice, condition (2.2.13) is considered sufficient in order to define the linear mode. ε_1 must be made large enough to take care of the inaccuracies in the system.

The operations to be performed by the switching circuit are summarized in the following table.

Input		Output
$U(\theta_e, \dot{\theta}_e) < 0$	$\left\| \theta_e \right\| > \varepsilon_1$	$-A$
$U > 0$		$+A$
$U > 0$	$\left\| \theta_e \right\| < \varepsilon_1$	0
$U < 0$		0

Table 2.1 Logic Operations of the Switching Circuit

As described earlier, the factor (M) in (2.2.12) has to be altered slightly. The function which is fed to the switching circuit is not $U(\theta_e, \dot{\theta}_e)$, but $U_a(\theta_e, \dot{\theta}_e)$. The function $U_a(\theta_e, \dot{\theta}_e)$ is not zero during the deceleration period. This fact could allow a simplification of the switching circuit by eliminating the memory. However, for the purpose of the present investigation it was felt that more time should not be spent in redesigning the circuit. In Table 2.2, the logic operations performed are shown.

Input	Gate	Output
$U_a(\theta_e,\dot{\theta}_e) < -\gamma$	$\lvert\theta_e\rvert > \varepsilon_1$	- A
$U_a(\theta_e,\dot{\theta}_e) > +\gamma$	$\lvert\theta_e\rvert > \varepsilon_1$	+ A
$U_a < -\gamma$	$\lvert\theta_e\rvert < \varepsilon_1$	0
$U_a > +\gamma$	$\lvert\theta_e\rvert < \varepsilon_1$	0

Table 2.2 Logic Operations of Actual Circuit

The threshold (γ) is adjustable to improve further the stability from noise. The peak-to-peak amplitude of the noise coming from the analogue computer is usually in the vicinity of 4 volts, which sets the value of γ and ε_1.

2.3.4 Design of the switching circuit.

In logic terminology, the switching circuit is an "AND" circuit (Figure 2.9) whose output (y) is the product of the two inputs restricted to take the values 0 and 1.

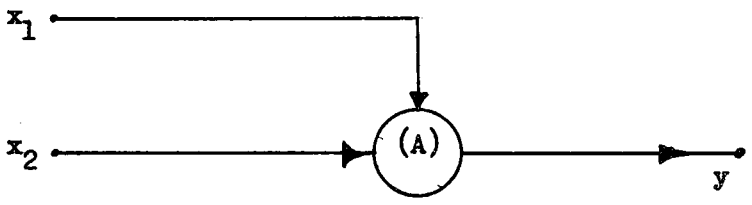

Fig. 2.9 "AND" Circuit

The simplified block diagram for the positive signals channel is shown in Figure 2.10. A more complete block diagram

appears in Figure 2.11. The circuit diagram is found in Appendix A-2.

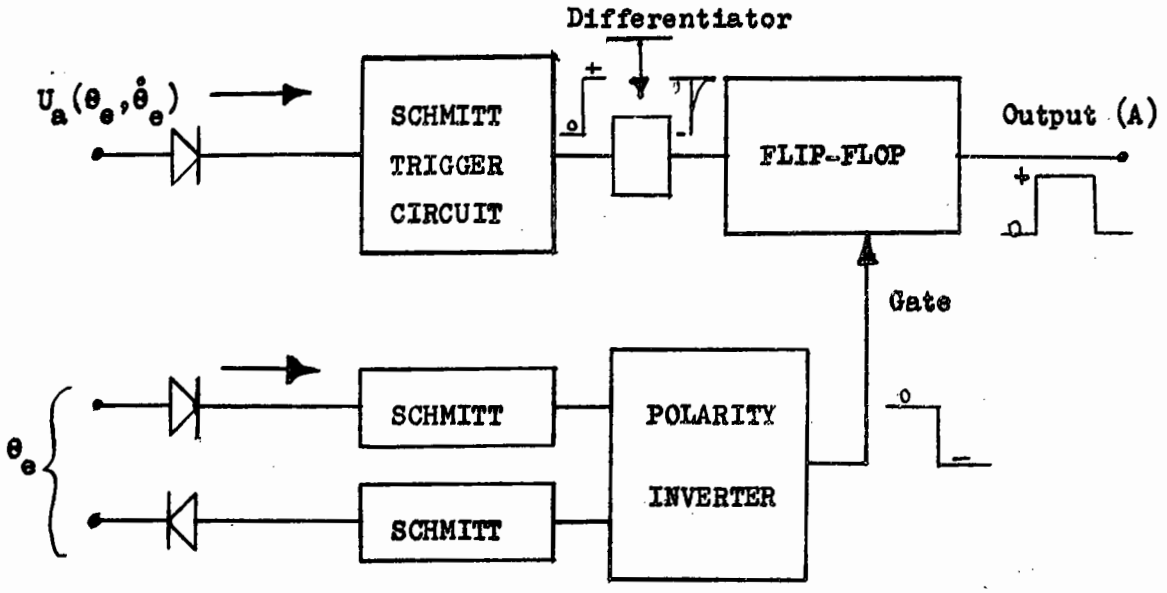

Fig. 2.10 Simplified block diagram of one channel of the switching circuit.

The core of the circuit is the Schmitt trigger (or level comparator) which gives a positive step output voltage when the "firing" level (γ or ε) is reached. After polarity inversion, the step is differentiated before being applied to the flip-flop. The latter is triggered only by a negative pulse injected at the plate of the "off" tube. The plate of the other tube is under the control of the trigger voltage of the second channel. In this fashion, the two flip-flops cannot be in the same state except when the gate is acting. The output is taken from the plate of the second tube. The gate voltage, also generated by a Schmitt trigger, is a negative voltage applied to the grid of the first tube of the flip-flop in order to hold it in the "off" state. The output (A) of the switching circuit is not fed

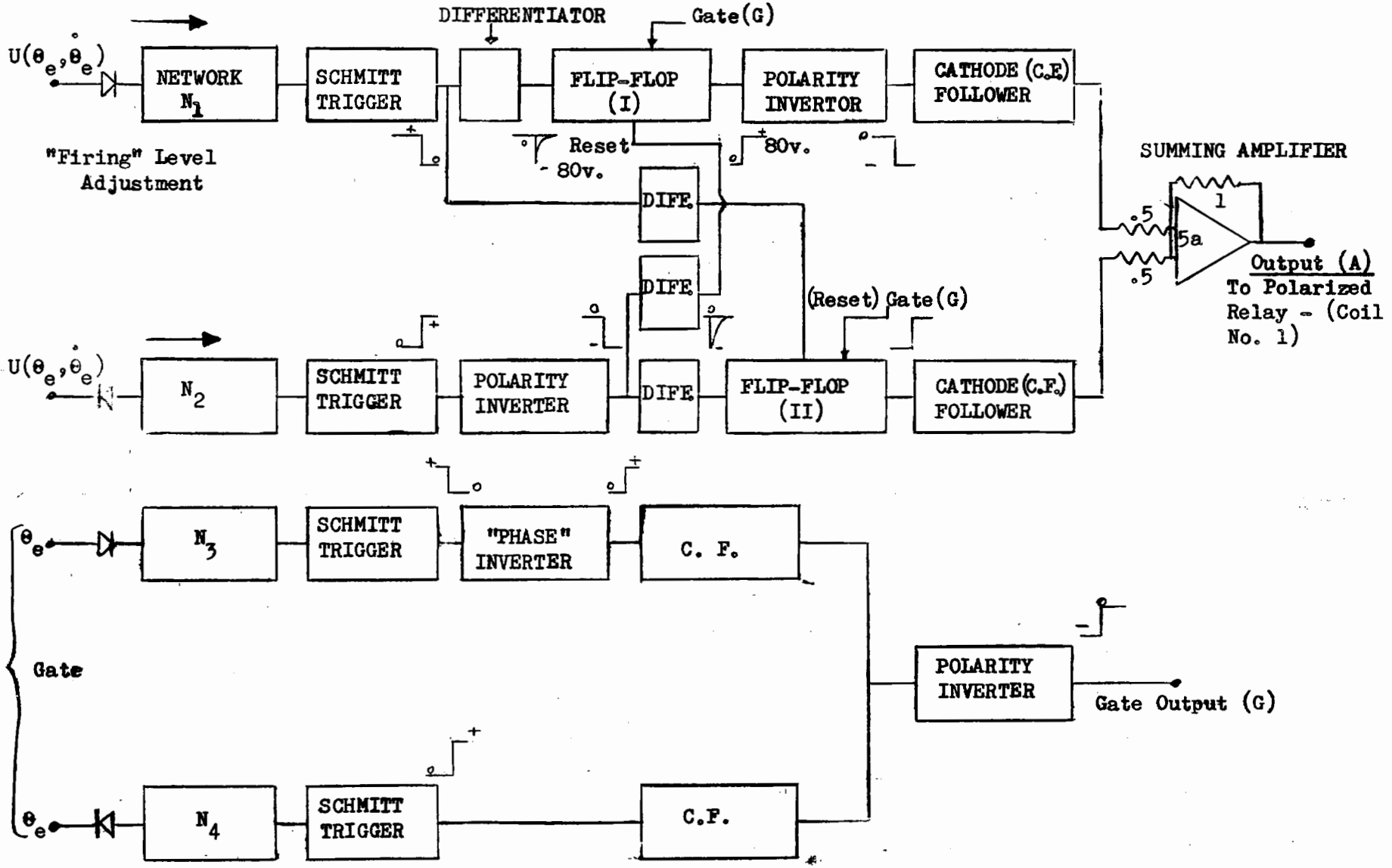

Fig. 2.11 Block Diagram of the Switching Circuit.

directly to the polarized relay of Figure 2.8 because in the off state the output voltage of the flip-flop is not exactly zero. This bias would constitute a secondary input producing a steady-state error in the oscillating servo during the linear mode. It is cancelled easily through the use of a summer amplifier of the Donner Analogue Computer.

The complexity of the circuit comes from the fact that it operates on d.c. voltages, hence the necessity of many polarity inverters, phase inverters and cathode followers to prevent the loading of the schmitt triggers and of the flip-flops.

Predictor.

The function of the predictor (Figure 2.7) is to generate the non-linear function $U(\theta_e, \dot{\theta}_e)$. In the present investigation, the predictor is constituted by the diode function generator and the operational amplifiers of the Donner Analogue Computer, Model 3000. The operational amplifiers are found very convenient in adding and subtracting the d.c. voltages in the servo loops. Certain precautions had to be taken, however, to prevent the generation of self-oscillations in the computer. The transients generated by the relays had a tendency to initiate oscillations. By using a second Donner Computer (10 amplifiers), it was possible to arrange the connections in order to prevent this state of affairs.

The non-linear function of velocity $f(\dot{\theta}_e)$ as generated by the computer is given in Appendix A-3. This function has been computed by Caswell using the following parameters for a gear ratio 18/1.

$$J = 2.12 \times 10^{-2} \text{ slug ft.}^2$$

$$T = 4 \times 10^{-1} \text{ lb. ft.}$$

$$F = 9 \times 10^{-3} \text{ lb. ft./rad./sec.}$$

Switching circuit in operation.

In Figure 2.12 is given the complete diagram of connections of the d.c. operational amplifiers used in the servo loop. Figure 2.13 shows the switching function $U_a(\theta_e, \dot{\theta}_e)$ and the output (A) of the switching circuit. The output of the latter in response to a triangular input with the gate circuit disconnected and $\gamma = \pm 5$ volts, is given in Figure 2.14. A general view of the equipment, the relay power controller and the switching circuit on experimental chassis are shown in Figures 2.15, 2.16 and 2.17 respectively. The transient response of the dual-mode systems appear in Chapter IV.

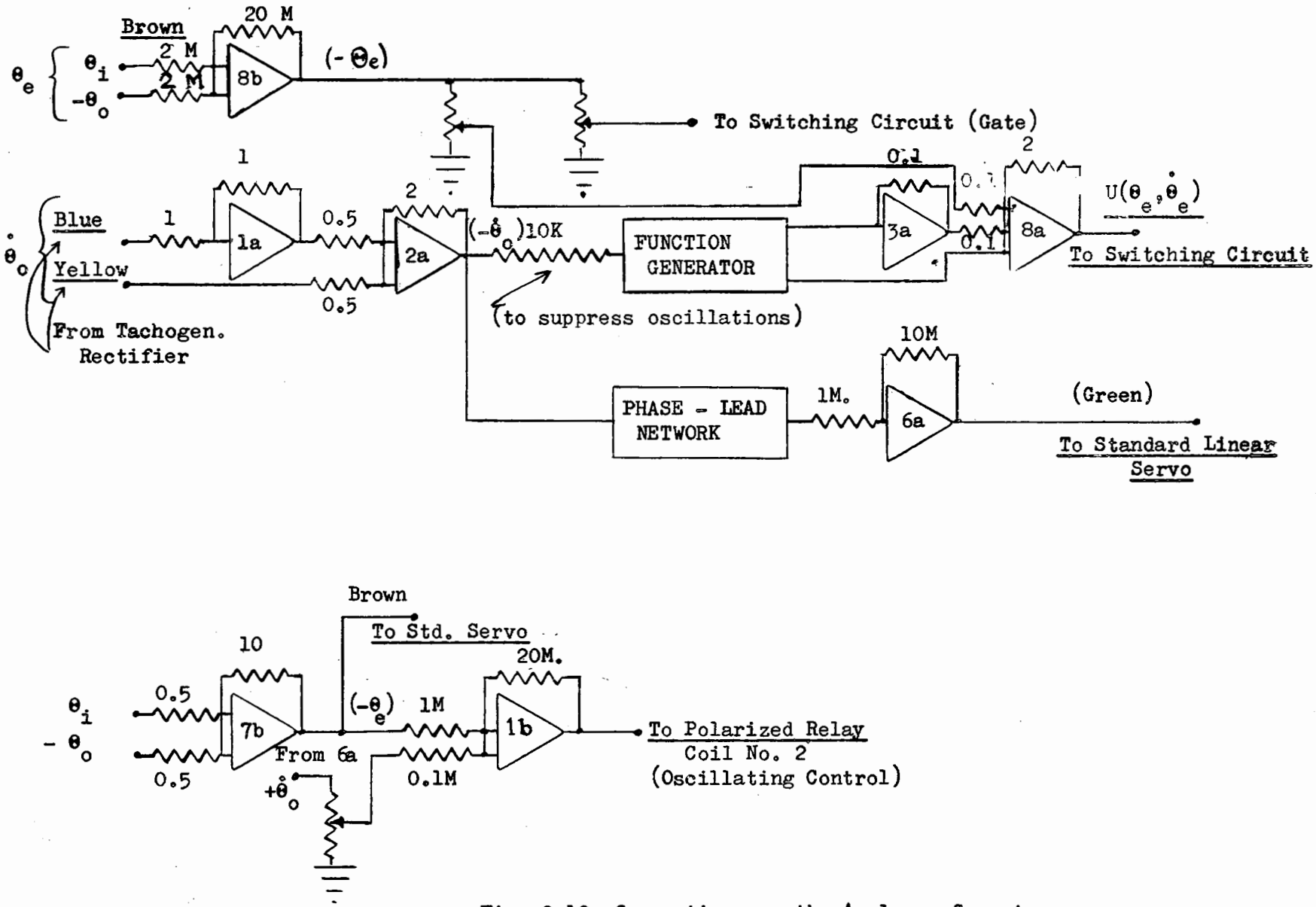

Fig. 2.12 Connections on the Analogue Computers

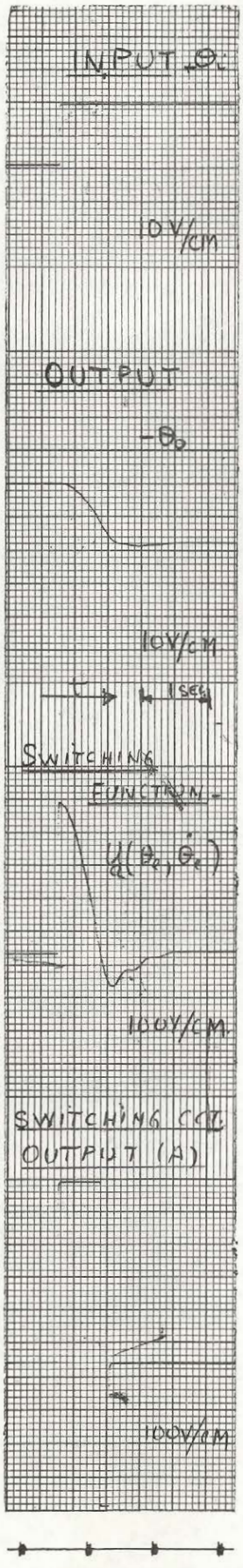

Fig. 2.13 Operation of a Dual-Mode System.

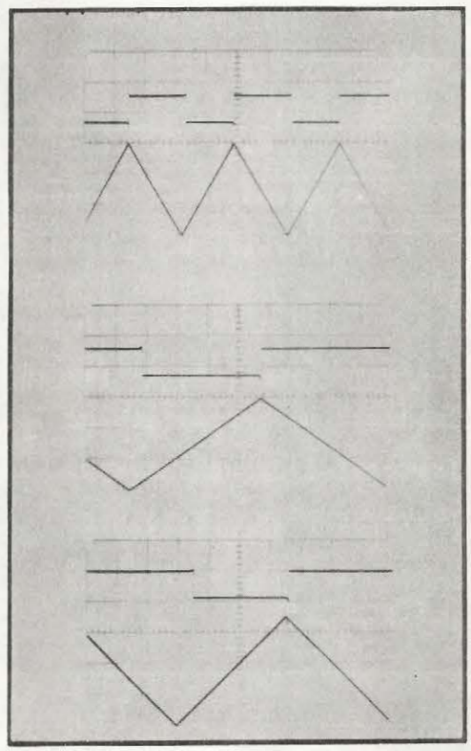

Fig. 2.14 Output (A) of the Switching Circuit in Response to a Triangular Input Showing Memory (Hysteresis) Effect.

No gate signal.

SCALES:

A. Input: 5 v/cm.
Output: 200 v/cm.
Sweep: 5 millisec./cm.

B. Input: 5 v/cm.
Output: 200 v/cm.
Sweep: 2 millisec./cm.

C. IDEM

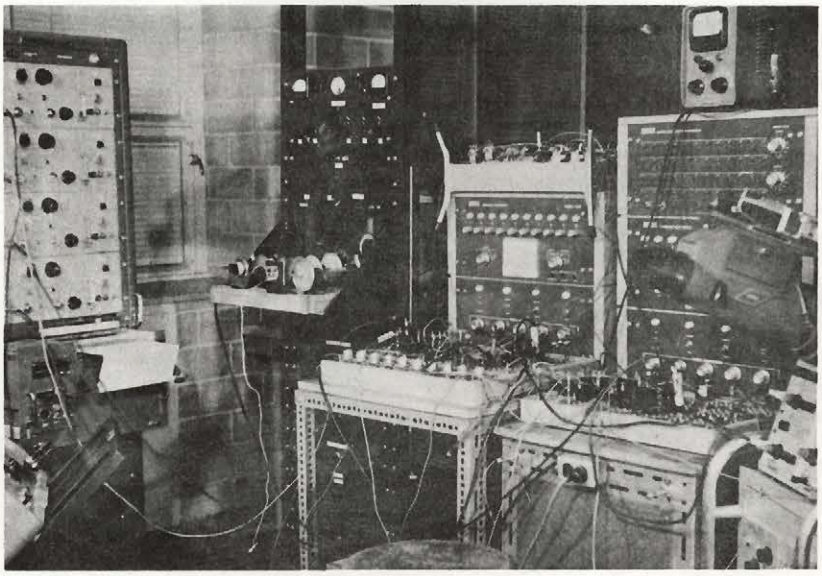

Fig. 2.15 General View of Equipment

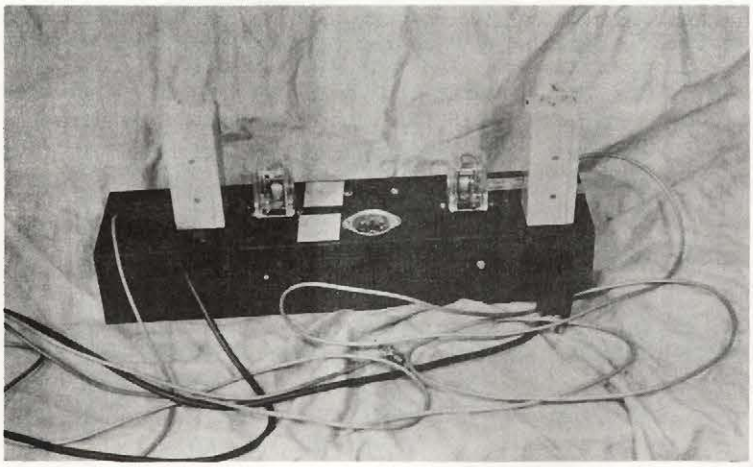

Fig. 2.16

Relay Power Controller

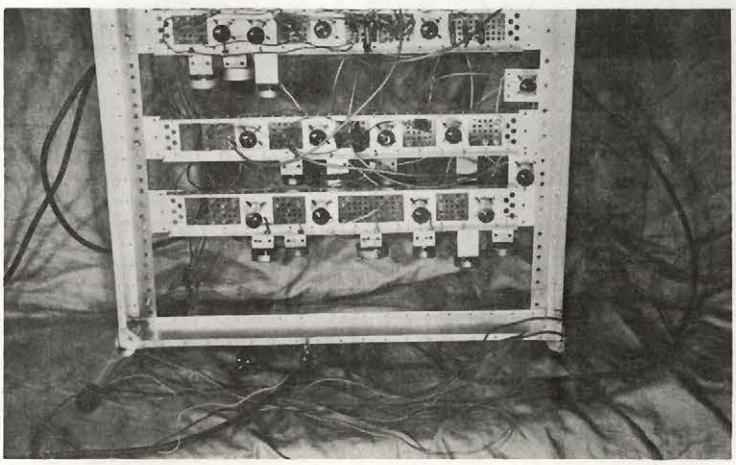

Fig. 2.17
Switching Circuit
on Experimental
Chassis

Chapter III

STUDY AND DESIGN OF THE DUAL-MODE PROGRAMMED SERVO LINEAR MODE

3.1 Introduction.

In the previous chapter, it was shown that any practical on-off servo is in fact of the dual mode type due to the presence of dead-zone. The steady-state behaviour of the programmed servo is, as in the simple relay servo, a limit cycle oscillation with finite frequency and amplitude. MacColl discovered that the steady-state oscillations are not objectionable because they produce an effective linearization of the relay output under certain conditions. This discovery demonstrated that there is no significant difference between an improved relay servo and the so-called "linear" type which exhibits saturation in its amplifiers and other components. In the present investigation, it was felt that the oscillating or carrier controlled relay amplifier would be the only logical controller to use in the linear mode of a dual-mode programmed servo. In this fashion, it is possible to remove the main objection against dual-mode systems; namely, their complexity. The carrier-controlled-dual-mode programmed servo constitutes a homogeneous entity.

This chapter covers a theoretical discussion of the carrier-controlled servomechanism and its practical realization into an experimental laboratory model.

3.1.1 General oscillating control servomechanism.

The analysis made by MacColl (1945) was restricted to the linearization of a relay-output by means of a superimposed

oscillation. This method was generalized by Loeb who proved its validity for the case where the output of the non-linear device is a functional of the input. The linearization process is then still effective when the non-linearities include hereditary effects like hysteresis, backlash, etc.

The relation between output and input of a non-linear device has been given by Loeb[24] in the form of the following theorem.

Theorem.

Let $y = F(x)$ be a functional of (x); i.e., a number which depends not only upon the actual value, but equally upon the past values of x.

Let $x(t)$ be a given periodic function of time t, the period of which is T, and add to this function $x(t)$, a small number (ε).

(Y) is then a function of time (t) (the period of which is T) and of (ε), if the two following conditions are satisfied.

a. The functional $F(x)$ is such that there is only a finite number of first discontinuities.

b. $F(x)$ may be represented by a sequence of functions the determination of which changes for definite values of (x), or dx/dt. There exist but a finite number of these changes of determinations.

These limitations are no practical drawback since this class of functionals comprise all the functionals liable to be found in practice.

3.1.2 Fourier expansion of the output.

The output takes the form

$$Y(x+\varepsilon) = (a_o + b_o \sin \omega t + c_o \cos \omega t + \ldots) + \varepsilon(a_1 + b_1 \sin \omega t + c_1 \cos \omega t + \ldots) + \varepsilon^2(\ldots) + \varepsilon^3(\ldots) \qquad (3.1.1)$$

Where $\omega = 2\pi/T$

This expression is obtained by first taking the Taylor expansion of (y), if (y) is regular.

$$y(x,\varepsilon) = y(x) + \varepsilon\left(\frac{dy}{dx}\right)_x + \varepsilon^2 \frac{1}{2}\left(\frac{d^2y}{dx^2}\right)_x \ldots \qquad (3.1.2)$$

Where $\varepsilon \ll x$ (3.1.3)

The expansion (3.1.1) holds when (3.1.3) is satisfied and when enough filtering is provided to take care of the higher harmonics. In a servomechanism, the filtering is provided by the low-pass characteristic of the motor and load combinations.

The expression of the output $y(x,\varepsilon)$ shows that an effective modulation of the carrier $x(t)$ by (ε) has taken place. The non-linear device will then be called a modulator. A distinction must be made between even and odd modulators as shown below.

3.1.3 Even and odd modulators.

a. Even modulator.

An even modulator is such that

$$y(x) = y(-x)$$

$$\left(\frac{dy}{dx}\right)_x = -\left(\frac{dy}{dx}\right)_{-x}$$

Therefore $y(t) = y(t + \frac{T}{2})$

whence: $b_o = c_o = 0$

$$a_1 = 0$$

If $x(t)$ has a symmetrical waveform, then

$$\underset{\text{even}}{y(x,\varepsilon)} \approx \varepsilon(b_1 \sin\omega T + c_1 \cos \omega t \ldots) \qquad (3.1.4)$$

This is the expression of an amplitude modulated sine wave. The even modulator is used in conventional a.c. servomechanisms.

b. Odd modulator.

In this case, the modulator is such that

$$y(x) = -y(-x)$$

$$\left(\frac{dy}{dx}\right)_x = +\left(\frac{dy}{dx}\right)_{-x}$$

These conditions specify

$$a_o = 0$$

$$b_1 = c_1 = 0$$

So that

$$\boxed{y(x,\varepsilon) \underset{\text{odd}}{\sim} (b_o \sin \omega t + c_o \cos \omega t) + \varepsilon\, a_1 + \ldots} \qquad (3.1.5)$$

3.1.4 Relay modulator.

A relay is an odd modulator because its output changes sign for any reversal of polarity at the input. The output is therefore given by the expression (3.1.5). In a servomechanism, (ε) is the d.c. error voltage which the feedback tends to reduce to zero. Condition (3.1.3) is then usually satisfied near the steady-state. $x(t)$ is a sweep oscillation.

In a servomechanism, the error $\varepsilon(t)$ has certain frequency components. The Taylor series expansion shows that the frequency of (ε) does not come into account since no derivative of (ε) is being used. However, it must be remembered that the expansion is correct only if the perturbation (ε) is small compared to the amplitude of the sweep $x(t)$.

In order to understand how small (ε) should be, it is necessary to study the response of a relay modulator when $\varepsilon(t)$ is given as a sine wave. This analysis has been done by MacColl[21] and repeated by Tsien[7].

Let $x(t) = E_o \sin \omega_o t$

$$\varepsilon(t) = kE_o \sin \omega t$$

The output of the relay is a width-modulated square wave of amplitude A

$$y(x,\varepsilon) = \sum_{m=0}^{\infty} \sum_{n=-\infty}^{n=+\infty} a_{nm} \sin (m\omega_o + n\omega)t \qquad (3.1.6)$$

For small (k), the two important coefficients are

$$a_{01} \approx \frac{4A}{\pi}$$

$$a_{10} \approx \frac{2Ak}{\pi} \qquad (3.1.7)$$

For general values of (k) these coefficients were computed by Kalb and Bennet[31].

When $0 < k < 1$

$$a_{01} = \frac{8A}{\pi^2} E(k)$$

$$a_{10} = \frac{8A}{\pi^2 k} \left[E(k) - (1-k^2) K(k) \right] \qquad (3.1.8)$$

where K(k) and E(k) denote the complete elliptic integrals of the first and second kind respectively. When k is small, the elliptic integrals can be expanded.

$$a_{01} = \frac{4A}{\pi} \left(1 - \frac{k^2}{4} - \ldots\right)$$

$$a_{10} = \frac{2Ak}{\pi} \left(1 + \frac{k^2}{8} + \ldots\right) \qquad (3.1.9)$$

It should be interesting to compute the deviation between (3.1.7) and (3.1.9) for $k = \frac{1}{2}$ and $k = \frac{1}{4}$.

$$k = \frac{1}{2}\,, \quad \triangle a_{01} = 7\% \qquad \triangle a_{10} = 4\% \tag{3.1.10}$$

$$k = \frac{1}{4}\,, \quad \triangle a_{01} = 1.5\% \qquad \triangle a_{10} = 0.8\%$$

The output of the relay is to a good approximation

$$y(x,\varepsilon) \approx a_{01} \sin \omega_o t + a_{10} \sin \omega t \tag{3.1.11}$$

$$y(x,\varepsilon) \approx \frac{2A}{\pi}\left[(2 - \frac{k^2}{2} - \ldots) \sin \omega_o t + k(1 + \frac{k^2}{8} - \ldots) \sin \omega t\right]$$

It is recalled that the input is

$$x(t) + \varepsilon(t) = E_o \sin \omega_o t + k \sin \omega t$$

3.1.5 Gain of the relay amplifier.

The gain for the sweep signal is

$$G_x = \frac{2A}{\pi E_o}(2 - \frac{k^2}{2} \ldots) \tag{3.1.12}$$

The gain for the error signal is

$$\boxed{G_\varepsilon = \frac{2A}{\pi E_o} \cdot (1 + \frac{k^2}{8} + \ldots)} \tag{3.1.13}$$

Those two gains are sketched against (k) in Figure 3.1.

In Figure 3.1 the following observations can be made:-

a. The error gain G_ε is relatively constant for values of up to $k \approx \frac{3}{4}$

b. The sweep gain (G_x) is affected more by an increase in (k) than is (G_ε). This is due to the increase in harmonics.

c. For moderate values of k, the error gain (G_ε) is 6 db lower than the sweep gain (G_x).

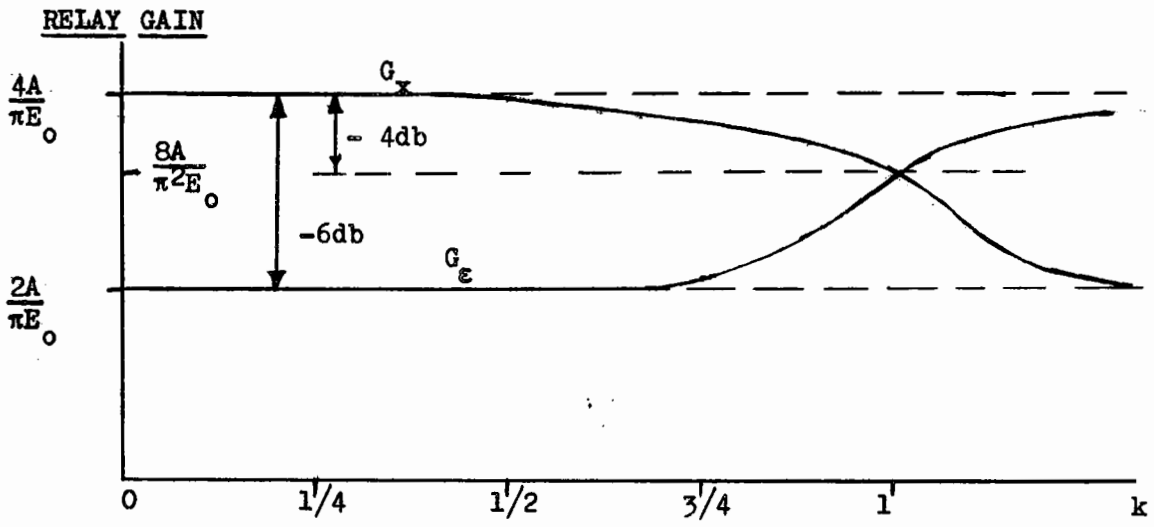

Fig. 3.1 Variation of $G_\varepsilon(t)$ and G_x with k

d. The gains (G_ε) and (G_x) are independent of frequency as long as (k) is small.

e. The gain (G_x) must be interpreted with care. For an ideal relay the fundamental component of the sweep in the output is independent of the amplitude (E_o).

f. The limit value of the fundamental frequency sweep amplitude in the output when $k \to 1$ is found by substituting in (3.1.8) the limits

$$E(k)_{k\to 1} \longrightarrow 1$$

$$(1-k^2)\, H(k)_{k\to 1} \longrightarrow 0$$

$$\text{Limit } a_{01} = \lim. a_{10} = \frac{8A}{\pi^2}$$

This value is a close approximation since, when $k = 1$ and $\omega \ll \omega_o$, the relay does not oscillate anymore and the output is $y = A$.

g. The oscillating relay amplifier is similar to a physical linear amplifier which has a region of non-linearity and saturation. There is one important difference, however. In the non-linear region the gain of the relay amplifier increases with the input signal.

h. The signal gain of the relay amplifier is inversely proportional to the amplitude (E_o) of the sweep signal x(t).

3.2 Application of the Relay Amplifier to a Position Servomechanism.

If the sweep or carrier x(t) is supplied from an external source, it is possible to select its frequency (f_o) to be much higher than the phase cross-over frequency (f_c) of the servo. The component in the relay output having the frequency (f_o) can then be filtered out quite effectively. The only signal that will be transmitted around the loop will be the error signal $\varepsilon(t)$. It is therefore possible to neglect the carrier frequency (f_o) altogether and to deal with the servo entirely by procedures normally applied to ordinary linear systems. Lozier[22] used this approach to design an oscillating servomechanism which he named "Carrier-Controlled Relay Servo".

The sweep signal can also be generated internally. The conditions for self-oscillation have been given in (2.2.15) and (2.2.16). The system will oscillate at a frequency (f_o) such that the total lag phase shift in the loop is πr. The amplitude (E_o) of these oscillations will adjust itself to make the loop gain 0 db at the frequency (f_o). There is no feedback correction for an error signal at that frequency, and (f_o) is therefore inherently above the frequency range for which the servo can successfully operate.

The following results can be derived from (3.1.5) when the servo has a single loop (no velocity feedback $\dot{\theta}_o$).

a. In the self-oscillating condition, the loop-gain to error signal is automatically set to give a 6 db loss at the phase cross-over frequency ($f_o = f_c$) of the Nyquist diagram of the system (Figure 3.2). Let the open loop error transfer function be

$$\frac{\bar{\theta}_o}{\bar{\varepsilon}} = F(j\omega) \qquad (3.2.1)$$

The open-loop transfer function for the carrier will then be

$$\frac{\bar{\theta}_o}{\bar{x}} = 2F(j\omega) \qquad (3.2.2)$$

The condition for self-oscillation is

$$2F(j\omega_o) = -1 \qquad (3.2.3)$$

Whence

$$F(j\omega_o) = -\frac{1}{2} \qquad (3.2.4)$$

The gain margin at the cross-over frequency controls the stiffness of the system. A 6 db gain margin is considered as optimum for a linear system. Reducing it (or increasing the stiffness) tends to deteriorate the dynamic tracking accuracy (or the accuracy in following rapidly varying signals), because the transient response is highly underdamped. In other words, the stiffness of the system sets the maximum slope of the ramp-input to which the servo can respond. On the other hand, reducing the stiffness spoils the static tracking accuracy (or accuracy in following a slow varying input). The velocity lag error increases. This error is due to the presence of viscous friction (F) and takes the value $\frac{F\omega_1}{k}$ for a ramp-input having a slope of ω_1 (Figure 3.2).

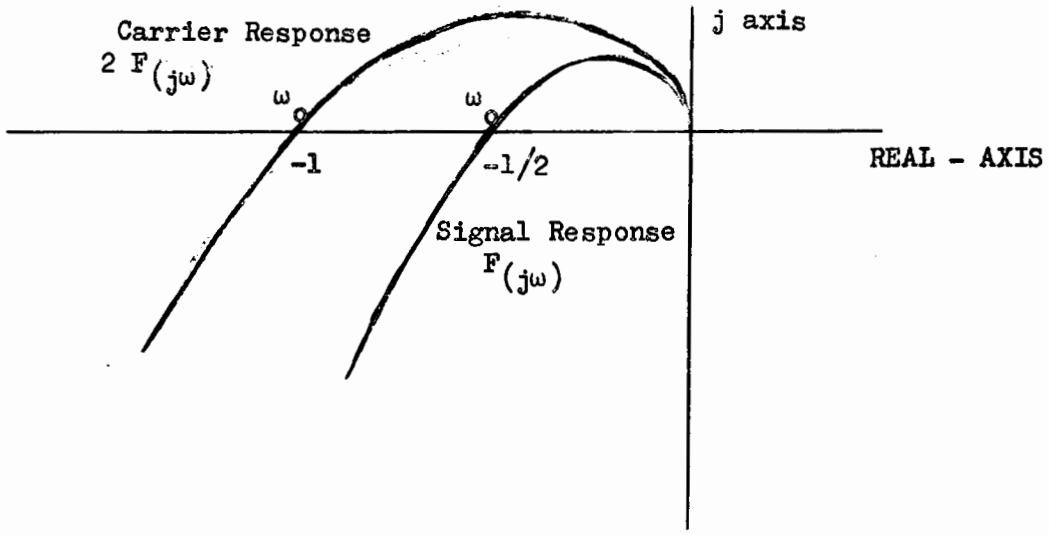

Fig. 3.2 Nyquist diagram of a carrier-controlled relay servo.

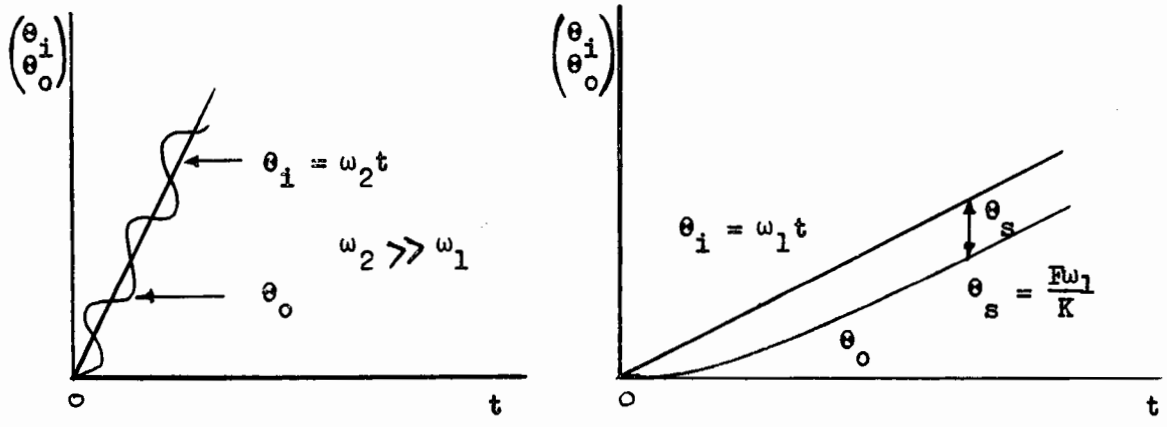

Fig. 3.3 Tracking performances of a servo.

If the amplitude of the input signal of frequency (f_o) is large, then it is seen in Figure 3.1 that the gain margin becomes -4 db. This means that a transient of large amplitude will take more time to die out in a carrier-controlled system

than in a conventional linear one. Let it be recalled, however, that in the system under investigation, transients of large amplitude fall under the control of the on-off mode. Lozier suggests the use of a saw-tooth sweep signal in order to prevent the reduction in the gain margin at higher amplitudes.

b. The use of an external sweep allows a linear control of the loop gain by the adjustment of the carrier amplitude. Its frequency (f_o) must be higher than the frequency (f_c) of the self-oscillations and its amplitude must be high enough to prevent the existence of such oscillations.

It can be said in conclusion that the carrier-controlled system can be designed to give the same flexibility and quality of performance as a conventional one while retaining the simplicity and the efficiency a relay servo.

3.2.1 External sweep versus internal sweep.

The advantages of using an external sweep can be summarized as follows.

a. The frequency (f_o) of the oscillations can be selected to be high enough in order to make the output ripple negligible. This frequency is limited however by the mechanical properties of the relays. In the present system, the maximum was about 15 c/s.

b. The loop gain can be adjusted by the carrier amplitude (E_o).

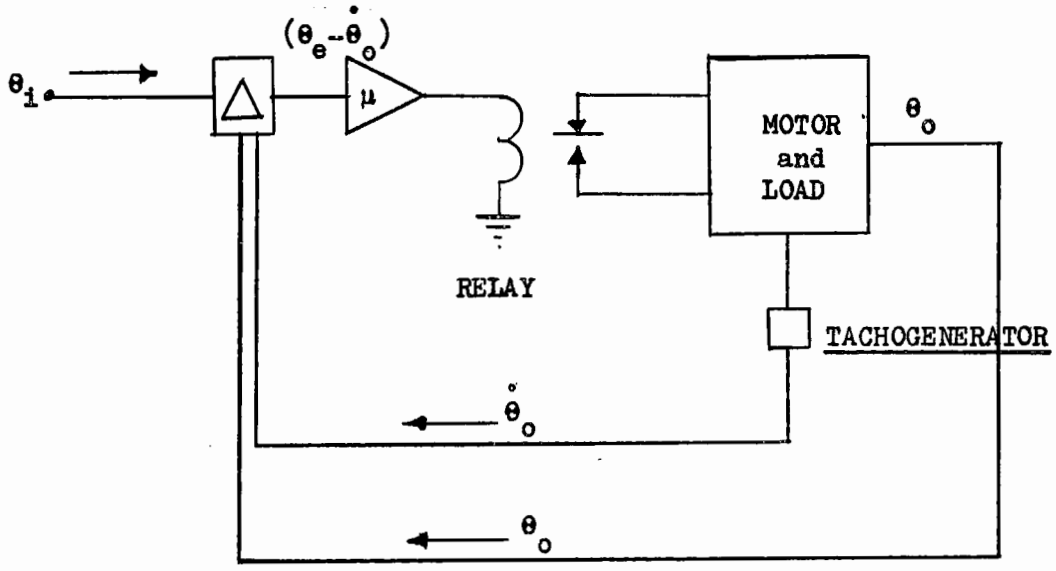

Fig. 3.4 Carrier-controlled relay servo with velocity feedback.

When the carrier is self-generated, the following conclusions can be drawn.

a. The loop gain for error signals adjusts itself automatically to an optimum value. This property is particularly useful when the relays have a threshold of operation, because their pull-in (or pull-out) voltage is finite.

b. The output ripple is usually more pronounced than when the carrier is supplied externally. Certain adjustments of gain can be made to reduce it to a minimum. For the majority of applications the small ripple is quite tolerable. In fact, it increases the static accuracy of the servo which is usually degraded by backlash and static friction. The ripple oscillates about a mean position which gives the

output position with great accuracy. This principle has been applied with success to high precision instrument servos as those described by Loeb[24].

It can be concluded that the servo with internal sweep has decidedly many advantages over the servo with externally applied sweep. Finally, it is more elegant and practical.

3.2.2 Control of the frequency of the self-oscillations.

As shown in Chapter II, the frequency of oscillation will increase if phase lead is provided in the servo loop. This phase lead can be produced by a network giving error-plus-error rate $(\theta_e + k\dot{\theta}_e)$ control. In simpler systems like this one, it is provided by velocity $(\dot{\theta}_o)$ feedback. The velocity feedback at the same time increases the viscous damping in the system. It has, however, the adverse effect of increasing the velocity lag error $(F\omega_1/K)$.

3.2.3 Control of the amplitude (θ_o) of oscillation when the relay has a threshold.

The amplitude of oscillation will set itself at the value (E_o) such that the carrier loop gain (g_ℓ) will be unity. The loop gain (μ) is proportional to the product of the d.c. amplifier gain (μ) times the true relay gain G_x' times the attenuation $\left|y(j\omega_o)\right|$ of the motor and load combination.

$$g_\ell = K_1 \mu \cdot G_x' \cdot \left|y(j\omega_o)\right| \qquad (3.2.5)$$

As discussed in Chapter II, article 2.2.5, the presence of a relay threshold decreases the relay gain by the factor $\sin \alpha$.

$$G_x' = G_x \sin \alpha \qquad (3.2.6)$$

where $$\text{Cos } \alpha = \frac{\varepsilon_o}{E_o} \qquad (3.2.7)$$

(ε_o) is the pull-in voltage of the relay which, as a simplification, is assumed to be equal to the pull-out voltage. Therefore, there is no phase-shift produced by relay hysteresis. Hence

$$g_l = K_1 \mu \, (G_x) \sin (\alpha) \left| y(j\omega_o) \right| \qquad (3.2.8)$$

Suppose that while the servo is oscillating the gain (μ) of the d.c. amplifier is decreased. It must be remembered that the output amplitude (θ_o) of the output oscillations of a relay servo using an ideal relay depends only on the frequency (f_o) and the applied torque $T = K_2 A$. The change in (μ) does not affect the frequency since the loop phase lag stays constant. Therefore, the only factor that will change in Equation (3.2.8) in order to bring the loop gain (g_l) back to unity is (sin α). The amplitude (E_o) of the self-oscillation will increase. If the relay had some hysteresis, the change in (μ) would make the system oscillate at a lower frequency, increasing (E_o) for the same reason.

In summary, it can be said that the relay threshold affects the amplitude of the oscillation, and the relay hysteresis affects its frequency. As a consequence, (μ) must always be very large. In the present system, (μ) is larger than 400.

3.3 Practical Realization of the Carrier-Controlled Amplifier.

The oscillating relay amplifier is so simple that it requires no design of any special equipmental. In the experiment set-up, the d.c. amplifier (μ) was conveniently replaced by an operational amplifier of

the Donner Analogue Computer, Model 3000. The gain (μ) is the ratio of feedback resistance R_f over input resistance R_i.

$$\mu = - R_f/R_i \qquad (3.3.1)$$

The relay system is the same one used in the on-off mode and shown in Figure 2.8 of Chapter II. The oscillating signal is applied to the second coil of the two coil polarized relay. Another operational amplifier serves as the error detector. The connection diagram is shown in Figure 3.5.

3.3.1 Component characteristics.

The complete circuit diagram of the relay power controller is found in Appendix A-1.

The power relays are operated by two 45 v. batteries controlled by the polarized relay. These components have the following characteristics.

a. Power Relays.

Potter and Brumfield, Type KCP11

Contact arrangement	DPDT
Coil resistance	R = 5000 ohms
Operating current	I = 5 ma.
Operating time delay	τ_0 = 10 ms (measured with Beckman Counter)
Release time delay	τ_R = 1 ms (measured with Beckman Counter)

b. Polarized Relay.

Type N.E. 280-EG

Contact arrangement	SPDT
Coil resistance	$R_1 = R_2$ = 1000 ohms
Operating current	I = 0.3 ma

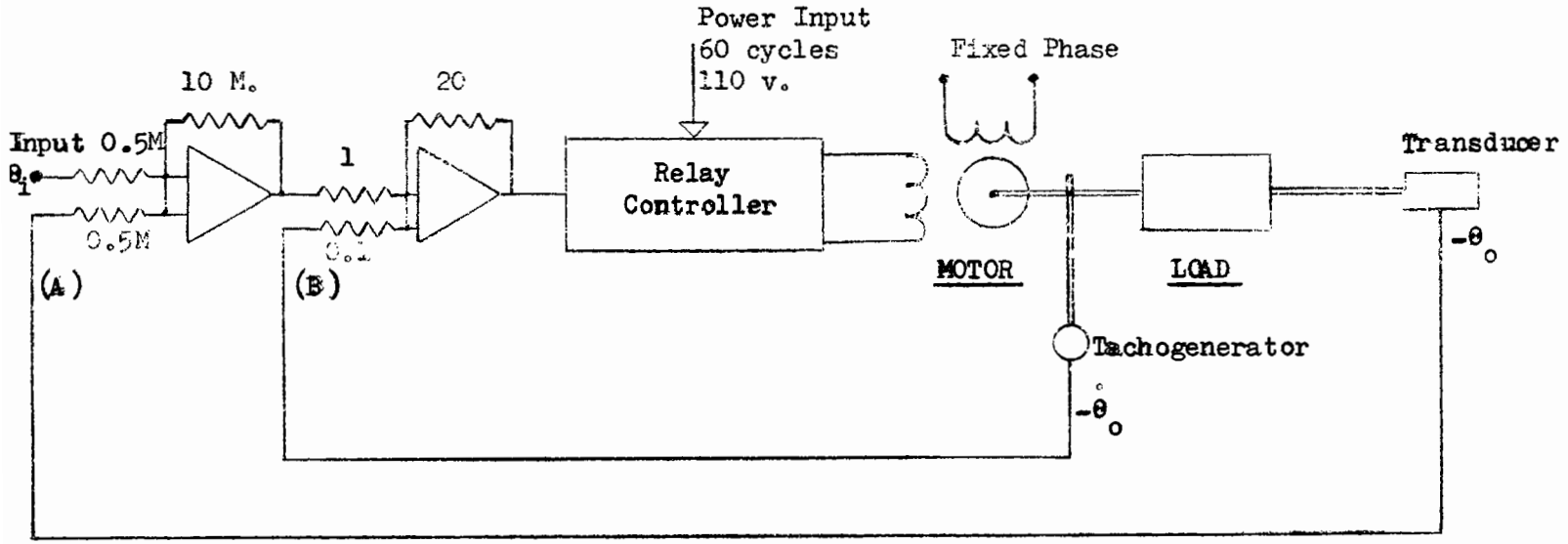

Frequency of Oscillation : f_o = 5.0 c/s

Output Position Signal (A) : (θ_o)= 0.1 volt peak-to-peak

Output Velocity Signal (B) : $(\dot{\theta}_o)$= 1.2 volt peak-to-peak

═══ Mechanical Connections

_____ Electrical Connections

Fig. 3.5 Self-Oscillating Carrier Controlled Relay Servo.

Operating time delay τ = 1 ms.

Note: No release spring - Number of coils = 2

3.3.2 Interaction of the control signals.

In Figure 2.8 it is seen that the first coil of the polarized relay is connected to the switching circuit. The second coil receives the carrier of the oscillating servo. The output voltage of the switching circuit is much larger than the amplitude of the carrier. In this fashion, coil No. 1 has control of the mode of operation as dictated by the switching circuit. The output of the latter should be zero for the linear mode. If instead, there remains a small residual voltage (α), its effect will be to magnetize the core of the relay in a certain direction. The result is the same as an additional error signal which the servo would then correct. As a consequence, the output of the servo would have a steady-state error having some relation to the extraneous input (α).

3.3.3 Qualitative study of the oscillating relay amplifier.

It is interesting to study qualitatively the output of an ideal relay operated by a signal $\left[E_o \sin \omega_o t + \varepsilon(t)\right]$ as shown in Figure 3.6 . The ideal relay is one which has no threshold and no time delay of operation. Its output is reversed when the sign of the input is changed.

The output torque is proportional to the relay output. When the error signal $\varepsilon(t)$ is zero, the relay output is a symmetrical square wave of amplitude A. When a signal $\varepsilon(t)$ is added to the carrier, the output becomes a non-symmetrical square wave having a definite d.c. level, with a polarity

depending on the polarity of $\varepsilon(t)$. The net output torque of the motor is proportional to this d.c. level.

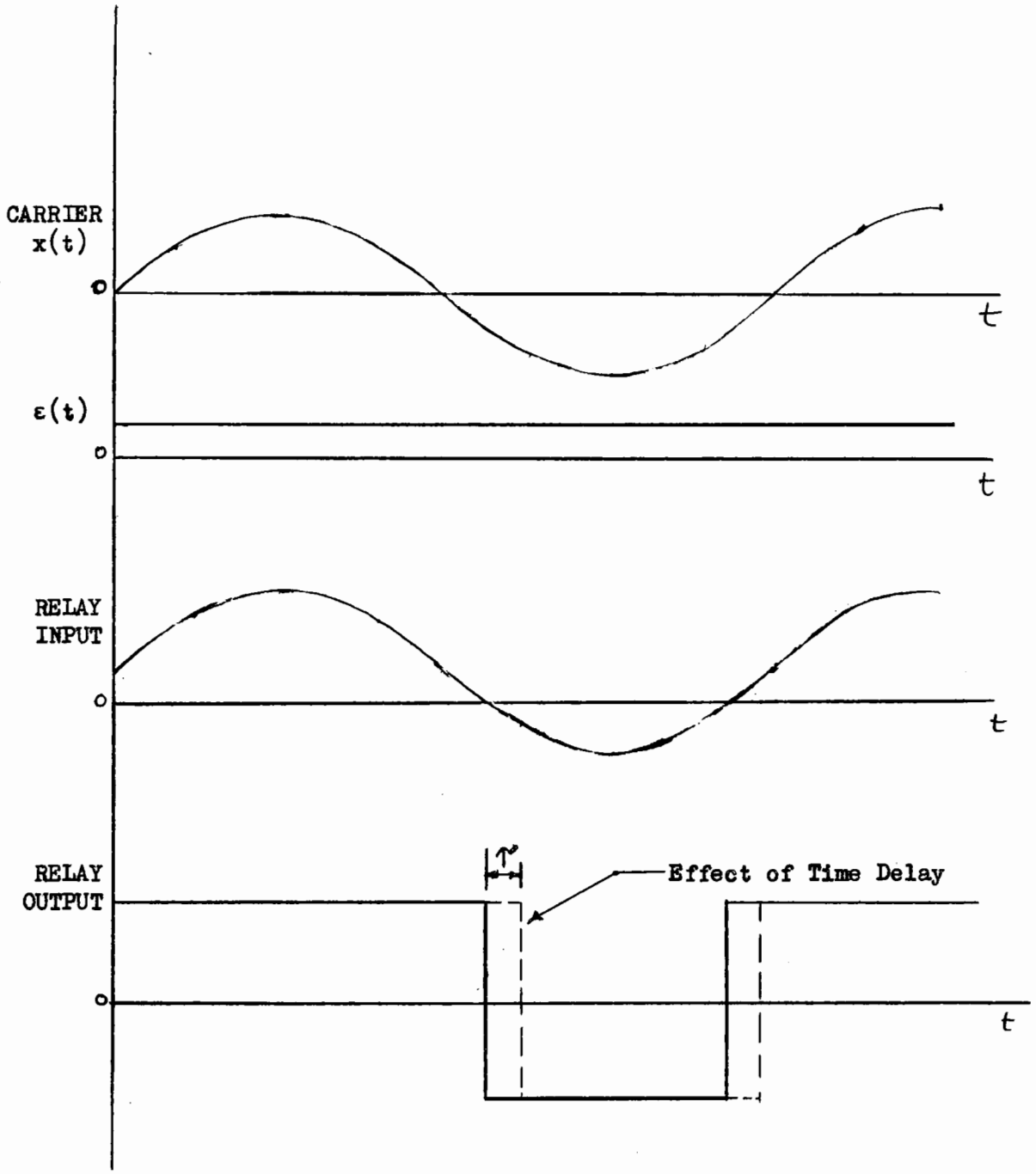

Fig. 3.6 Description of the operation of an oscillating relay amplifier.

Effect of time delay.

If the relay has an operating time delay τ_{sec}, its output will be a square wave of frequency (f_o), but it will be

lagging by τ seconds. This corresponds to a phase lag of $(\omega_0 \tau)$ for the fundamental component (Figure 3.6).

Effect of Threshold.

If the relay has a pull-in voltage ε_0 and a pull-out voltage of the same value, the output of the relay will appear as shown in Figure 3.7.

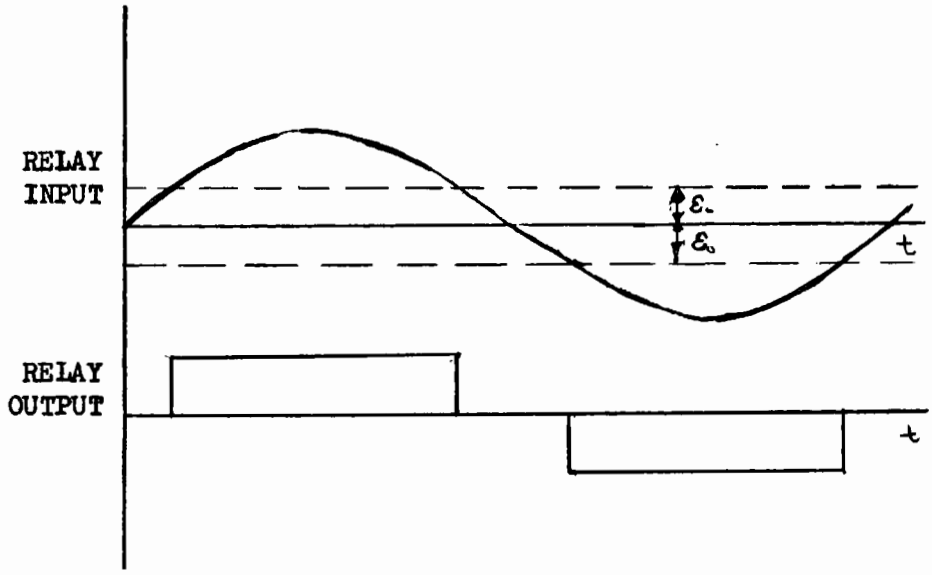

Fig. 3.7 Output of relay with threshold.

The consequence of the threshold is to reduce the amplitude of the fundamental component of the output. If the pull-out voltage differs from the pull-in voltage, there is in addition a hysteresis effect. The linearity of the carrier-controlled relay amplifier is not affected, however, by these added non-linearities.

The polarized relay used in the model servo has a negligible time delay ($\tau \approx 1$ ms). It has no release spring which makes its output have the appearance shown in Figure 3.8.

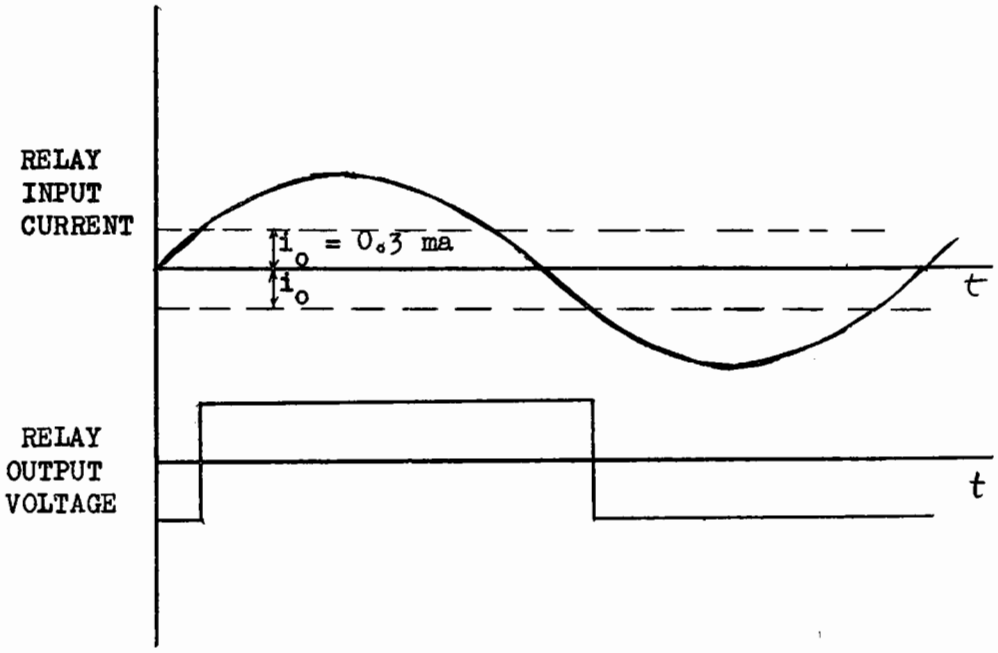

Fig. 3.8 Output of polarized relay N.E. - 280-EG.

The special characteristic of the polarized relay has the effect of a time lag (τ_1) which depends on the threshold and the amplitude of the carrier. No attenuation of the fundamental component is provided however. The amplitude of the input current should be as high as possible in order to obtain the maximum frequency for a given setting of all other parameters.

3.3.4 Performance of the carrier-controlled relay servo.

The performance of the carrier-controlled relay servo has been measured by its response to a step and a ramp input given in Figure 3.12, and its closed-loop frequency response shown in Figure 3.16. The direct measurement of the open-loop response is impossible because of the necessity of maintaining the self-oscillation.

For the purpose of simplification, the error-rate ($\dot{\theta}_e$) signal has been replaced by the output position velocity ($\dot{\theta}_o$)

readily available from the tachogenerator. The consequence of this is to increase the velocity lag error, which in fact has no importance in this investigation.

The frequency of the self-oscillations increases with the amount of velocity feedback. The self-oscillating servo has the following characteristics:

Minimum step-input to cause saturation	$\pm$ 4 volts
Frequency of oscillation	f_o = 5 c/s
Output oscillation amplitude	$\lvert\theta_o\rvert$ = 0.1 volts peak-to-peak
Amplitude of the velocity signal	$\lvert\dot{\theta}_o\rvert$ = 0.6 volts peak-to-peak
Velocity lag error (ramp-input)	θ_s = 0.48 volts. rad./sec.
Phase cross-over frequency ($\phi = 180^o$)	f_c = 5.0 c/s

Gain margin of the servo.

The gain margin is reduced by the velocity feedback signal. It is difficult to measure it directly due to the carrier oscillation. However, it can be calculated by reasoning as follows.

The carrier signal fed to the relays is proportional to the vector sum: $\bar{\theta}_o + \bar{\dot{\theta}}_o$.

Any sinusoidal command signal (θ_i) of frequency (f_o) will suffer a 6 db attenuation around the loop.

Now, as far as the relay amplifier is concerned, the command signal enters the loop as (θ_i) and comes out as ($\bar{\theta}_{01} + \bar{\dot{\theta}}_{01}$). This means that

$$\frac{\left|\bar{\theta}_{01} + \bar{\dot{\theta}}_{01}\right|}{\left|\theta_i\right|} = \frac{1}{2}$$

and, using the relation,

$$\frac{|\theta_{01}|}{|\bar{\theta}_{01} + \ddot{\theta}_{01}|} = \frac{|\theta_{0}|}{|\bar{\theta}_{o} + \ddot{\theta}_{o}|}$$

it is found that

$$\frac{|\theta_{01}|}{|\theta_{i}|} = \frac{1}{2} \times \frac{0.1}{\sqrt{(0.1)^2+(0.6)^2}} = 0.08$$

The open-loop gain is then

$$\left|\frac{\theta_o}{\theta_e}\right| = \left|\frac{1}{\frac{\theta_i}{\theta_o} - 1}\right| = \frac{1}{11.5} = 0.08$$

The closed-loop frequency response shown in Figure 3.1 has been sketched in the vicinity of the cross-over frequency. The open-loop gain at (f_c) can be guessed to be around 0.1. From Figure 3.15 the cross-over gain of the linear servo is found to be about (0.2) at 3.0 c/s. For purposes of comparison, the stiffness should be about the same. The above results show that this is about right. The two systems have been adjusted for almost identical velocity lag errors.

3.4 Characteristics of the Servo Components and of the Standard Linear Controller.

The model servo used in this investigation is of the a.c. type. It is powered by a two-phase, 60 cycle servo-motor driving an inertia load with a gear ratio of 18:1 as shown in Figure 3.9. The input and output position angles are translated into d.c. voltages by two 10-turn precision potentiometers. The output velocity is obtained from an induction tachogenerator giving a modulated a.c. output which is then rectified and amplified. The amplification of all d.c. voltages is done conveniently by the operational amplifier. All d.c. correction

voltages are transformed into a modulated 60-cycle signal. The modulation is of the suppressed carrier type. A phase shifting network produces a 90° phase shift necessary for the operation of the servo-motor. The modulated signal is passed through a preamplifier before being applied to the push-pull power amplifier. The linear controller composed of the modulator preamplifier and power amplifier is linear only over a limited range of input voltages. Outside that range there is a region of non-linearity and saturation.

The preamplifier had to be redesigned because it was loading the modulator so much as to necessitate a 20 db booster amplifier. The output hum has also been reduced. It was found that the rectified output of the tachogenerator had an important phase lag (45° at 0.5 c/s).

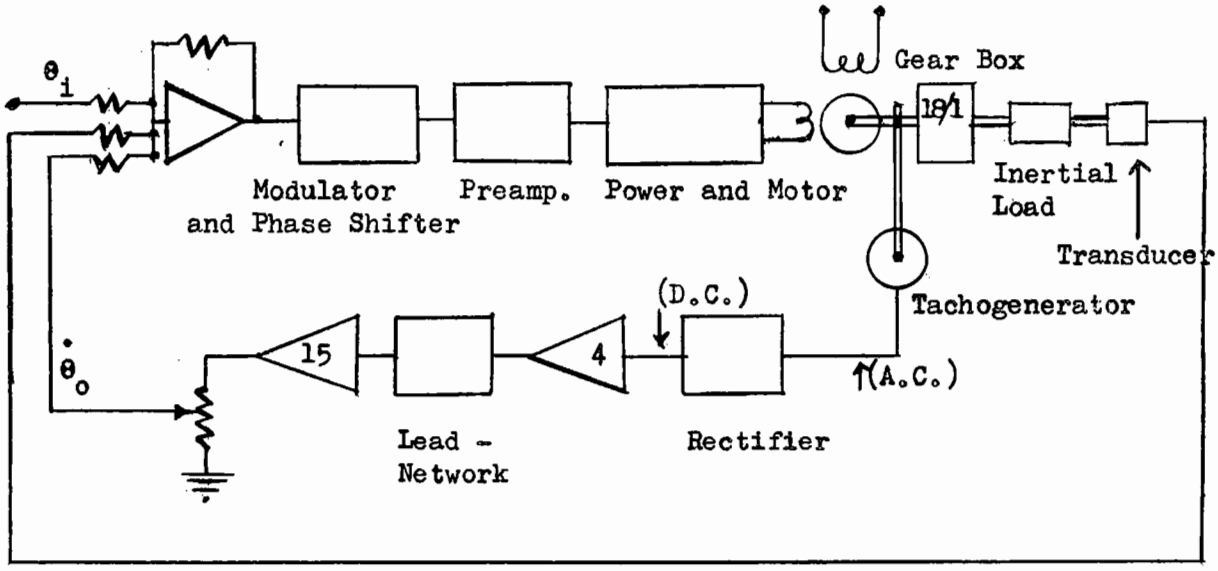

Fig. 3.9 Linear position servomechanism

3.4.1 Characteristics of the components.

The characteristics of the mechanical components are referred to the output shaft.

a. Transducers. The transducers are two 20 Kohm, 1%, 10-turn Spectrol potentiometers. Their output voltage is related

to the position angles by the following scale factor.

$$\theta_o = \frac{7}{27} \frac{\text{volts}}{\text{rad.}} \approx 1.11 \frac{\text{volt}}{\text{rad.}}$$

b. Tachogenerator. The tachogenerator is of the induction type. Its output is a modulated 60-cycle signal which is rectified in a phase sensitive rectifier and amplified. The d.c. output signal appearing at point (6) in Figure 2.2 is a linear function of the output velocity over a certain range.

$$\dot{\theta}_o(\text{volts}) = K \dot{\theta}_o \ (\text{Rad./sec})$$

Slope in the linear region:

$K = 3.61$ volts/rad./sec.

Limit of the linear region:

$\dot{\theta}_{omax} = \pm 49$ volts (3500 R.P.M. motor)

Correction network:

A phase lead network has been found necessary in order to correct for the phase lag introduced by the rectifier.

Phase lag $= 45^o$

$f_o = 0.5$ c/sec.

An attenuation of about 1:15 is introduced by the actual network. The circuit diagram is shown in Appendix A-4.

c. Servo-motor.

Type: 2-phase, 60 cycle, Diehl, FP-25-11

Maximum power output	5 watts
Maximum velocity	3500 R.P.M.

Maximum torque (V_c = 100 v)	4.5 oz. inches
Approximate torque speed slope (V_c = 100 v)	1.1×10^{-3} $\frac{\text{oz. in.}}{\text{R.P.M.}}$

d. System parameters.

All the parameters are referred to the output shaft. The viscous friction (F) is due to the torque-speed characteristics of the motor.

Gear ratio	18:1
Inertia	$J_0 = 2.12 \times 10^{-2}$ slug ft.^{2}
Viscous friction	$F_0 = 9 \times 10^{-3}$ lb.ft./rad./sec.
Maximum output torque	$T_{0max} = 4.1 \times 10^{-1}$ lb.ft.
Output torque	$T_0 = T_{0max} - F_0 \dot{\theta}_0$
Overall gain	$K = \frac{T_0}{\text{input to mod.}} =$ $0.209 \frac{\text{lb.ft.}}{\text{d.c. error volt}}$

e. Linear controller.

Maximum output power (500 ohm load)	= 50 watts
Maximum output voltage	= 175 volts R.M.S.
Corresponding d.c. input to modulator	= $\pm$ 4 volts d.c.
Corresponding a.c. input to power amplifier	= 3 volts peak-to-peak
Maximum linear output voltage	= 100 volts R.M.S.
Corresponding input to modulator	= $\pm$ 2 volts d.c.

The circuit diagram of the new preamplifier is found in Appendix A-5. More information about the linear servo is given by Caswell[29].

3.4.2 Nyquist diagram of the linear servo.

The linear servo has two feedback loops, one for the position signal, the other for the position velocity signal. Only the first loop was open for the Nyquist diagram of the servo. This was done in order to make a fair comparison with the oscillating servo. The two-loop system has been reduced into a single loop as follows.

Let the open-loop transfer function without velocity feedback be

$$\frac{\theta_o}{\theta_e} = KF_{(p)} \qquad (3.4.1)$$

With velocity feedback, the input becomes

$$\theta_e = \theta_i - \alpha P\theta_o \qquad (3.4.2)$$

Whence $$\frac{\theta_o}{\theta_i - \alpha P\theta_o} = KF_{(p)} \qquad (3.4.3)$$

where $$\alpha > 0 \qquad (3.4.4)$$

The equivalent one-loop system has a transfer function

$$G_{(p)} = \frac{\theta_o}{\theta_i}$$

$$G_{(p)} = \frac{KF_{(p)}}{1 + \alpha KPF_{(p)}} \qquad (3.4.5)$$

The block diagrams of the transformation are given in Figures 3.10 and 3.11

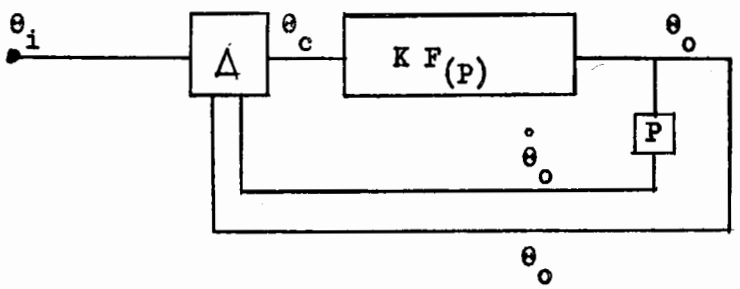

Fig. 3.10 Servomechanism with two feedback loops

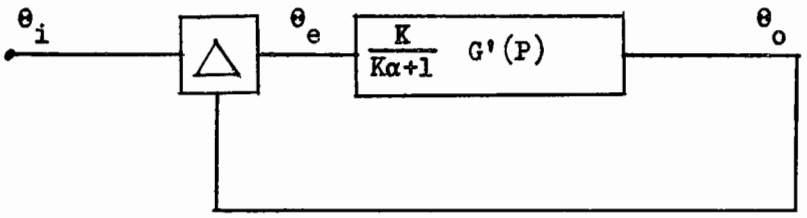

Fig. 3.11 Reduction of the two-loop system into a single loop.

$$\text{Let } F_{(p)} = \frac{1}{P(PT_1+1)(PT_2+1)\ldots(\quad)} \tag{3.4.6}$$

$$G_{(p)} = K \frac{1}{P(PT_1+1)(PT_2+1)} \cdot \frac{1}{1+K\alpha P/P(PT_1+1)(PT_2+1)}$$

$$G_{(p)} = K \frac{1}{P\left[(PT_1+1)(PT_2+1)+K\alpha\right]} \tag{3.4.7}$$

$$\text{Then } G_{(p)} = \frac{K}{K\alpha+1} \frac{1}{P(P^2 T_1T_2/K\alpha+1 + P(T_1+T_2)/K\alpha+1 + 1)} \tag{3.4.8}$$

$$\text{or } G_{(p)} = \frac{1}{(K\alpha+1)P(PT_3+1)(PT_4+1)} \tag{3.4.9}$$

It can be proved that

$$\frac{1}{T_3} + \frac{1}{T_4} = \frac{1}{T_1} + \frac{1}{T_2} \tag{3.4.10}$$

$$\frac{1}{T_3 \cdot T_4} = \frac{1}{T_1T_2} + K\alpha T_1T_2 \tag{3.4.11}$$

It can be concluded that the effect of the velocity feedback is to

a. decrease the velocity error coefficient K by the factor $(K\alpha+1)$.

b. decrease the larger time constant (T_1) and increase the smaller time constant (T_2).

The velocity feedback then increases the velocity lag error and tends to transform the two poles into a double pole. As a consequence, the Nyquist diagram, Figure 3.15, intersects the 180^{o} axis almost perpendicularly.

3.4.3 Measurement of the servo time constants.

In a single-loop servomechanism with no compensating network, the only time constants present are those of the motor and load combination. The main time constant is equal to the ratio (J/F) of the inertia to the friction damping factor. The second depends on the electrical characteristics. For example, in the case of a d.c. motor using constant armature current, it is the ratio (R/L) of the resistance of the field control winding to its inductance. T_1 and T_2 are, therefore, completely independent.

The measurements were made on the open-loop frequency response of the linear servo with no velocity feedback. The input sinusoidal voltage was kept within the linear region and recorded at the same time as the output on a two-channel Sanborn Recorder. It was found that much care was necessary in order to make phase measurements with an acceptable accuracy, especially at the high frequencies. The presence of noise caused the output position to drift, carrying the pen recorder off-scale. At low frequencies, the measurements were limited by the amplitude of the output oscillations. However, the accuracy was judged sufficient because only the order of magnitude of the time constants was necessary.

The two corner frequencies are measured on the Bode diagram (Figure 3.14). They are the frequencies where the phase

lags are 135° and 225° respectively since the separation between them is more than two octaves. In the present tests, the 135° point could not be measured. An estimate was made by sketching that section of the phase curve with an approximately constant slope of 18.4 degrees per octave in the vicinity of $\phi = 135^{\circ}$.

The results are:

Time constants.

$$\tau = \frac{1}{2\pi f}$$

$$\phi_1 = 135^{\circ}\ ,\ f_1 = 0.08\ c/s\ ,\ T_1 = 2.0\ sec. \qquad (3.4.12)$$

$$\phi_2 = 225^{\circ}\ ,\ f_2 = 3\ c/s\ ,\ T_2 = 0.053\ sec. \qquad (3.4.13)$$

Natural resonance frequency.

$$\phi_R = 180^{\circ} \qquad f_R = 0.6\ c/sec. \qquad (3.4.14)$$

3.4.4 Calculation of the time constants.

According to theory, the time constant (T_1) is given by

$$T_1 = \frac{J}{F} = \frac{2.12 \times 10^{-2}}{9 \times 10^{-3}} = \underline{2.36\ seconds} \qquad (3.4.15)$$

This result is not far removed from 3.4.12.

The second time constant, T_2, can be calculated from the slope at t = 0 of the phase plane diagram (Equation 2.2.4). This slope can be found by taking the effective applied torque to be

$$T = T_{max}\,(1 - e^{-\alpha t}) \qquad (3.4.16)$$

Then it can be proved that

$$\left.\frac{d\dot{\theta}_o}{d\theta_o}\right|_{t=0} = \alpha - \frac{F}{J} = \frac{1}{T_2} - \frac{1}{T_1} \qquad (3.4.17)$$

For a second-order system the initial slope is infinite.

The phase-plane diagrams are recorded from an oscilloscope (A, B, Chapter IV).

Slope measured.

$$\left.\frac{d\dot{\theta}_o}{d\theta_o}\right|_{t=0} = 62.5 \frac{\text{volts}}{\text{volts}} \frac{(\text{velocity})}{(\text{position})} \qquad (3.4.18)$$

Multiplying by the appropriate scale factors given above

$$\left.\frac{d\dot{\theta}_o}{d\theta_o}\right|_{t=0} = 62.5 \times \frac{1.11}{3.21} = 19.2 \text{ (1/sec.)}$$

$$\frac{F}{J} = 0.43 \text{ (1/sec.)}$$

Whence $T_2 = \frac{1}{\alpha} = \frac{1}{19.6} = \underline{0.051 \text{ sec.}}$ (3.4.19)

This result compares favorably with (3.4.13).

3.4.5 Adjustment of the damping factor.

In order to make a fair comparison with the carrier-controlled system, the damping factor of the linear servo was adjusted to give the same tracking error (velocity lag). This was done by feeding a ramp-input to the system and by observing both input and output signals on a dual-trace oscilloscope, Figure 3.13.

Velocity lag error.

a. Carrier-controlled servo

$$\varepsilon_s = 0.48 \text{ volt/rad./sec.}$$

b. Linear servo

$$\varepsilon_s = 0.52 \text{ volt/rad./sec.}$$

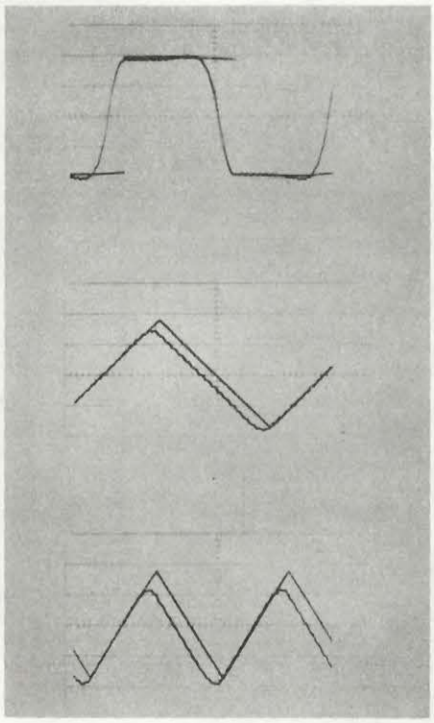

Fig. 3.12 Response of the Carrier-Controlled Relay Servo.

Vertical Scale: 2 v/cm.
Sweep: 1 sec./cm.

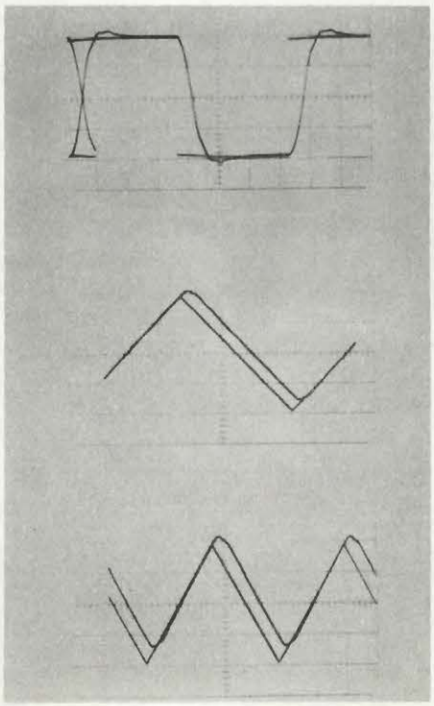

Fig. 3.13 Response of the Standard Linear Servo.

Vertical Scale: 2 v/cm.
Sweep: 1 sec./cm.

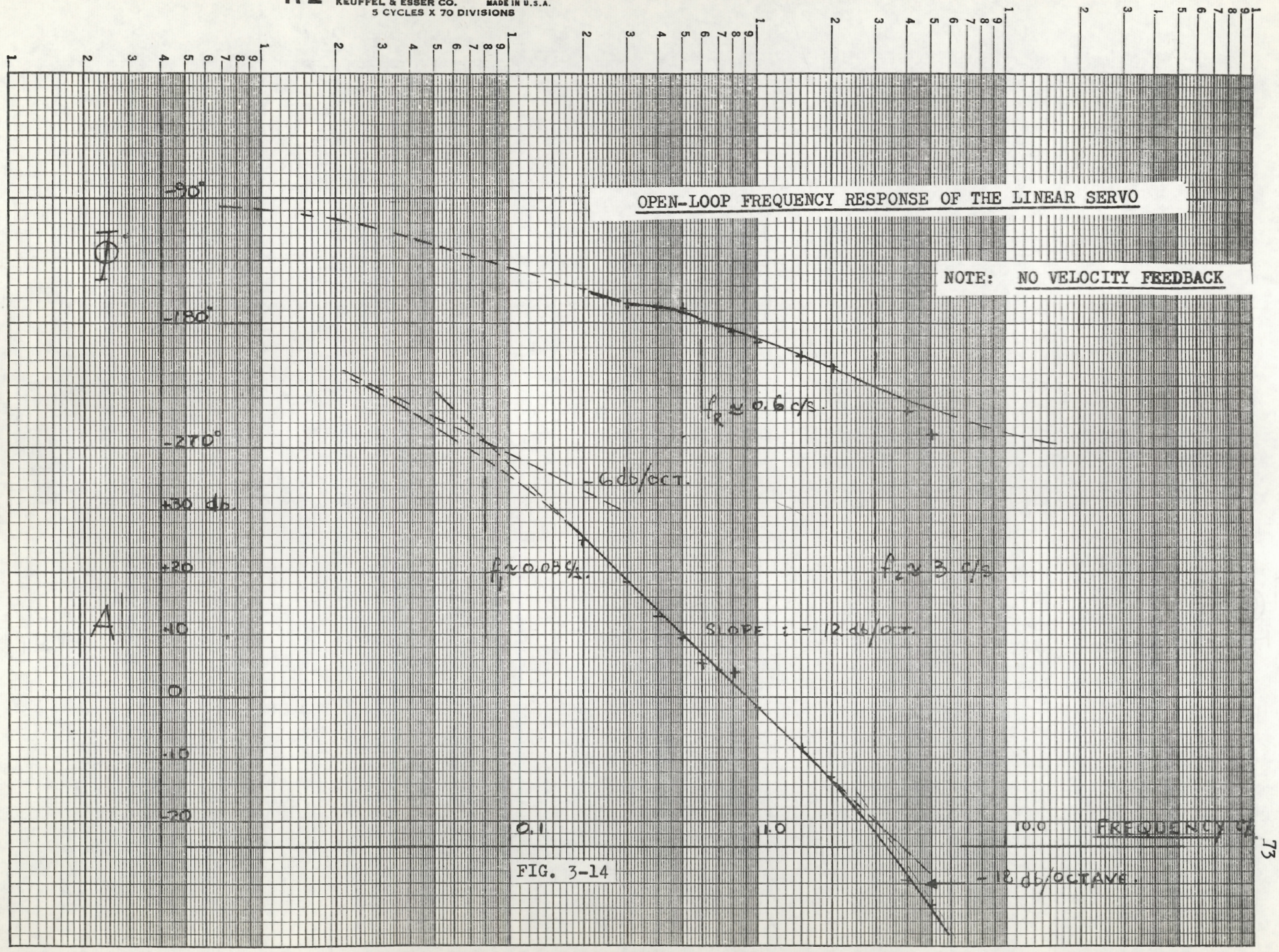
K&E SEMI-LOGARITHMIC 359-91
KEUFFEL & ESSER CO. MADE IN U.S.A.
5 CYCLES X 70 DIVISIONS
OPEN-LOOP FREQUENCY RESPONSE OF THE LINEAR SERVO
NOTE: NO VELOCITY FEEDBACK
-90°
-180°
-270°
+30 db.
+20
+10
0
-10
-20
0.1
1.0
10.0
FREQUENCY
$f_2 \approx 0.6$ c/s.
-6 db/oct.
$f_1 \approx 0.03$ c/s.
$f_2 \approx 3$ c/s
SLOPE : - 12 db/oct.
- 18 db/OCTAVE.

FIG. 3-14

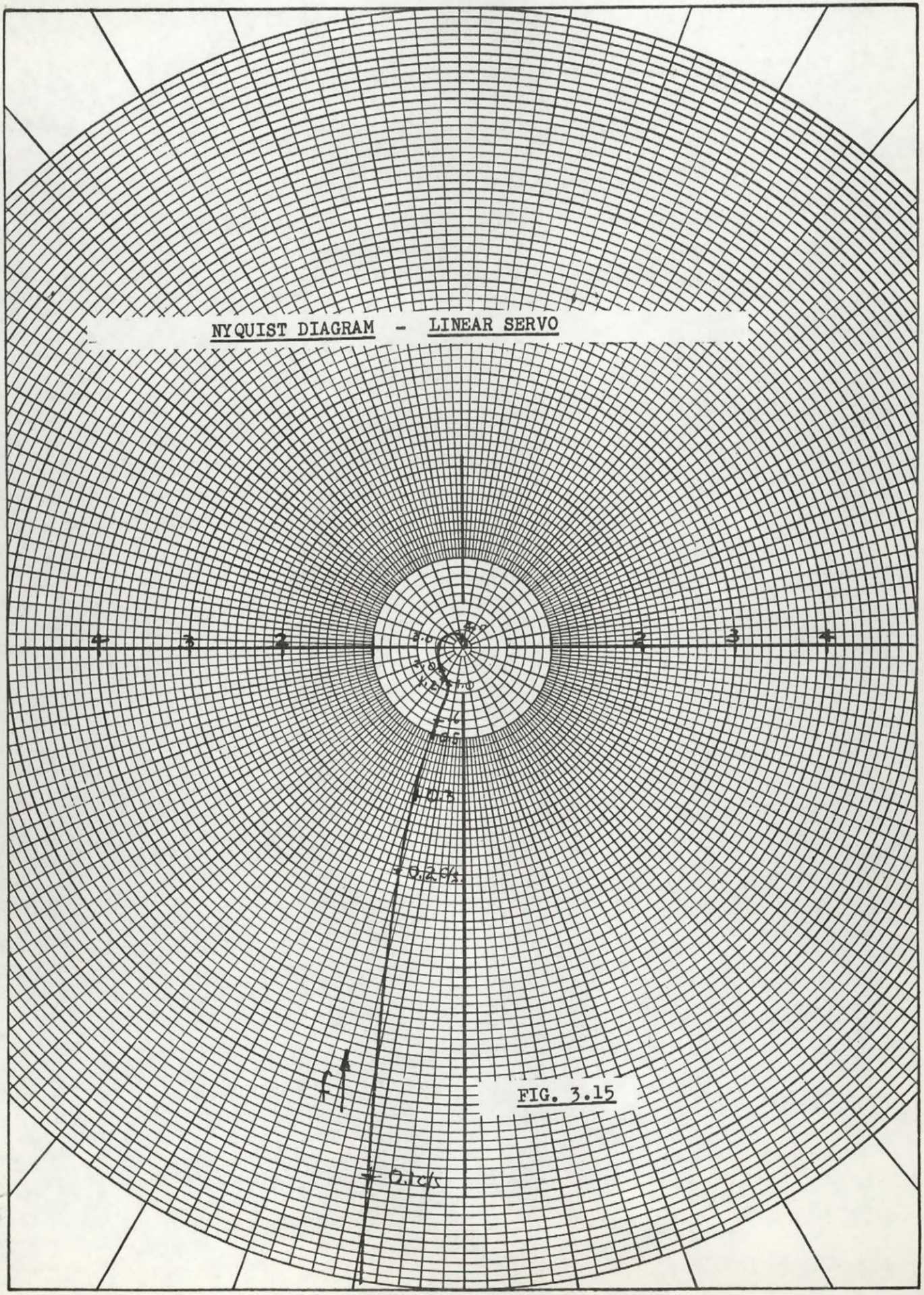
NYQUIST DIAGRAM - LINEAR SERVO
4
3
2
2
3
4
3.0
2.8
2.6
2.4
2.2
2.0
1.8
1.6
1.4
1.2
1.0
0.8
0.6
0.5
0.4
0.3
0.2
0.1

FIG. 3.15

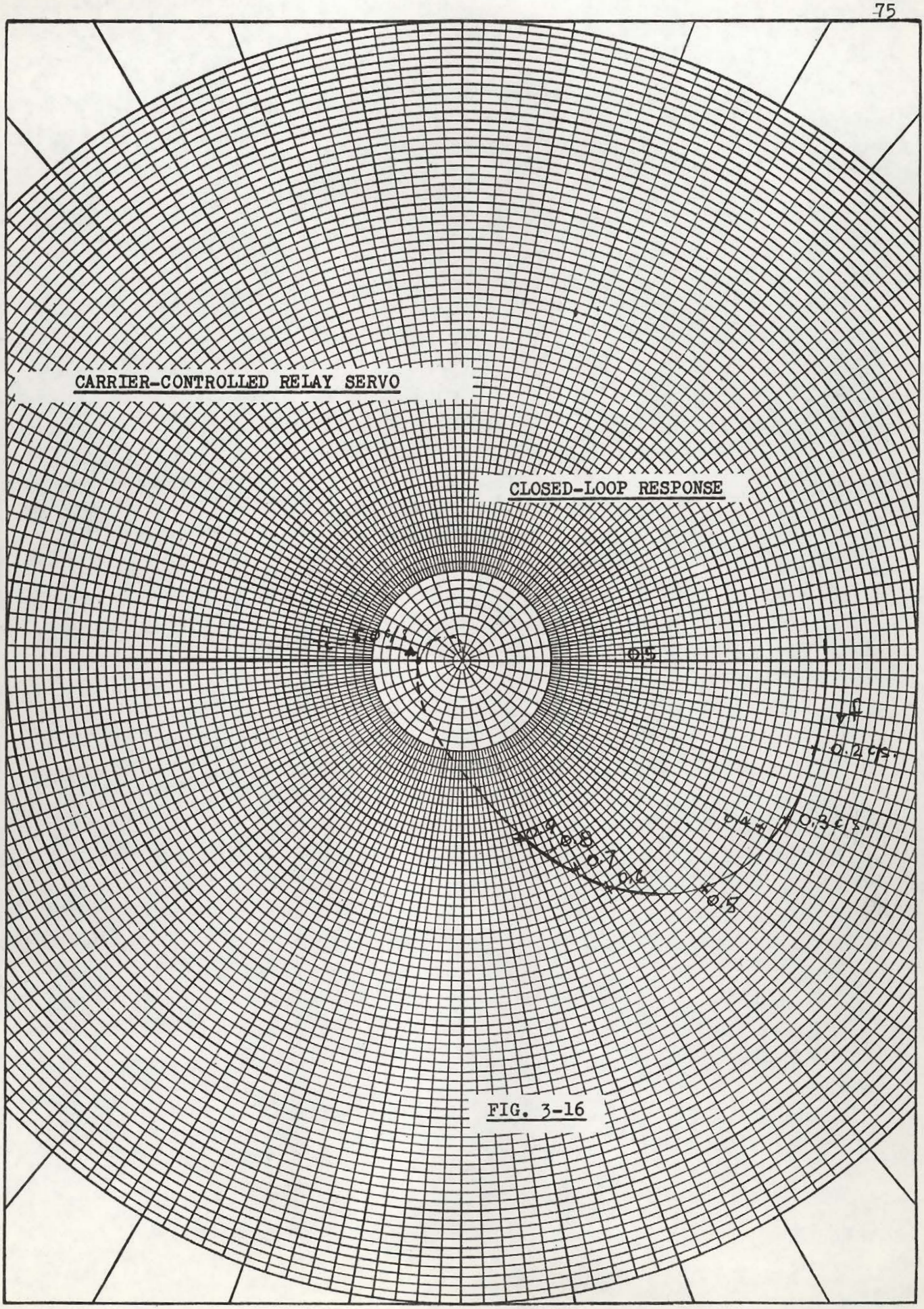
CARRIER-CONTROLLED RELAY SERVO
CLOSED-LOOP RESPONSE
0.5
0.4
0.3
0.2
0.9
0.8
0.7
0.6
0.5

FIG. 3-16

Chapter IV

EXPERIMENTAL RESULTS AND CONCLUSIONS

4.1 The purpose of the tests is to compare the transient performance of the model servo using four different controllers.

a. Dual-Mode Carrier-Control

b. Dual-Mode Standard Linear

c. Carrier-Control

d. Standard Linear

The responses are recorded as phase-plane diagrams on an oscilloscope, and as time functions on a pen recorder. The comparison is based on the response time.

4.1.1 Error Criterion.

When dealing with a true linear system, it is customary to define the time of response as the time taken to reduce the error from 90% to 10% of its initial value. In this fashion, the response time is independent of the magnitude of the step-input. This criterion does not take the amount of overshoot into account.

In the case of non-linear systems, it is better to define the time of response as the time taken by the servo to reduce the error from its initial value to a fixed small value ($\pm\varepsilon$) consistent with the accuracy of the system. In these tests, (ε) has been chosen as, $\varepsilon = \pm 0.2$ volt.

4.1.2 Tabulation of results.

The response time of the four different systems is given

in the form of a graph for step-inputs of various sizes in Figure 4.6. The same results appear in Table 4.1.

TYPE OF SYSTEM	STEP-INPUT	RESPONSE TIME	OVERSHOOT	REMARKS
	volts	seconds	volts	
Carrier-Control	3.3	1.1	0.0	
	9.0	1.6	0.2	Error causing saturation
	15.0	1.9	0.5	
	21.0	2.3	0.5	$\lvert\theta_e\rvert \geqslant$ 4 volts
	26.5	2.6	0.5	
Dual-Mode Carrier-Control	3.8	1.4	1.0 →	No saturated torque reversal
	9.0	1.5	0.8	
	15.0	1.8	0.5	
	21.0	2.0	0.3	Linear mode:
	27.0	2.4	0.5	
	28.5	2.2	0.2	$\lvert\theta_e\rvert <$ 1.0 v.
Dual-Mode Linear	3.6	1.0	0.3 →	No saturated torque reversal
	9.0	1.5	0.8	
	15.0	1.9	0.4	
	21.0	2.1	0.5	
	27.0	2.4	0.6	
Linear	1.8	0.8	0.0	Error causing Saturation
	4.0	1.2	0.4	
	9.0	1.1	0.2	
	15.0	1.9	0.4	$\lvert\theta_e\rvert \geqslant$ 2 volts
	21.0	2.3	0.5	
	26.5	3.0	0.5	

Table 4.1

4.2 Discussion of the Results.

4.2.1 Response-time and overshoot.

The first glance at Table 4.1 reveals that the differences between the four systems are not as marked as would be expected. In Figure 4.6 the same results are given in the form of graphs

- PHASE PLANE DIAGRAMS -

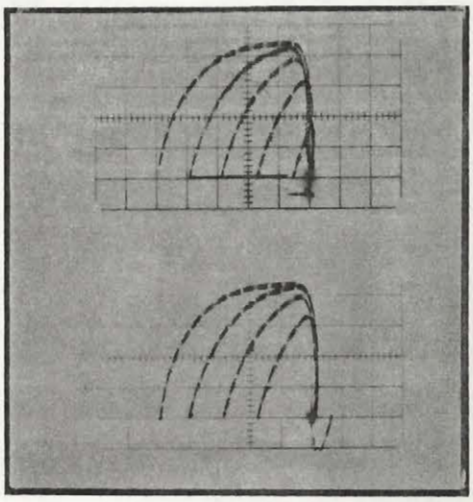

A. Dual-Mode - Linear

B. Dual-Mode - Carrier-Controlled

SCALES: Vertical ($\dot{\theta}_e$): 10 v/cm.
Horizontal (θ_e): 5 v/cm.

LINEAR MODE: $\varepsilon = \pm 1$ v.

Time Marker: 100 millisec.

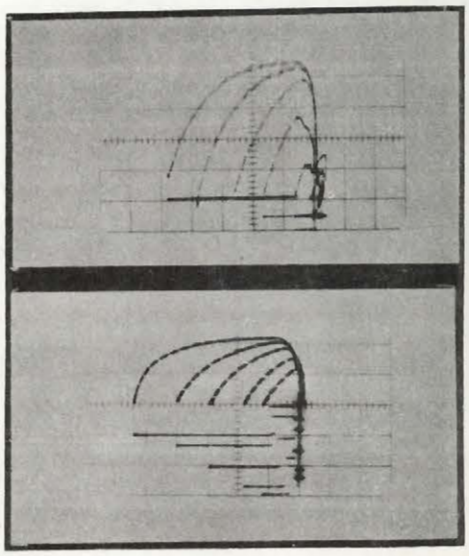

C. On-off with Dead-Zone

$\dot{\theta}_e = 10$ v/cm.
$\theta_e = 5$ v/cm.
$\varepsilon = \pm 1$ v.

D. Dual-Mode - Carrier-Controlled

Second trace is output (A) of switching circuit.

SCALES: $\dot{\theta}_e = 20$ v/cm.
$A = 200$ v/cm.
$\theta_e = 5$ v/cm.

LINEAR MODE: $\varepsilon = \pm 1$ v.

- PHASE PLANE DIAGRAMS -

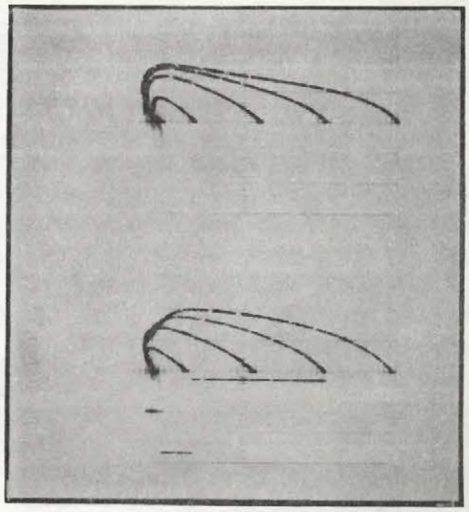

E. Standard Linear Servo

Saturation Input: $\pm$ 2 v.

F. Dual-Mode - Standard-Linear

Output (A) of Switching Circuit

Linear Mode: $\pm$ 1 v.

SCALES: Vertical $\dot{\theta}_e$ = 20 v/cm.

A = 200 v/cm.

Horizontal θ_e = 2.5 v/cm.

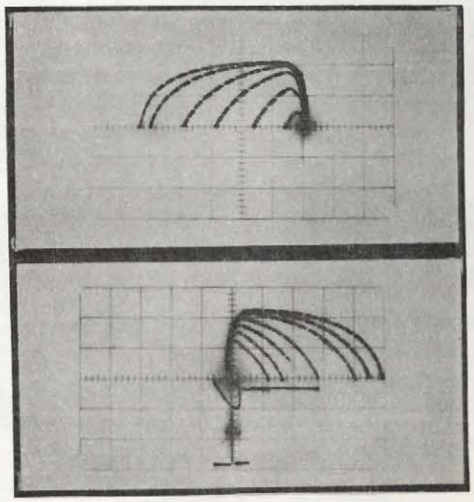

G. Carrier-Controlled Relay Servo

Saturation Input: $\pm$ 4 v.

H. Dual-Mode Carrier-Controlled Relay Servo

SCALES: $\dot{\theta}_e$ = 20 v/cm.

θ_e = 5 v/cm.

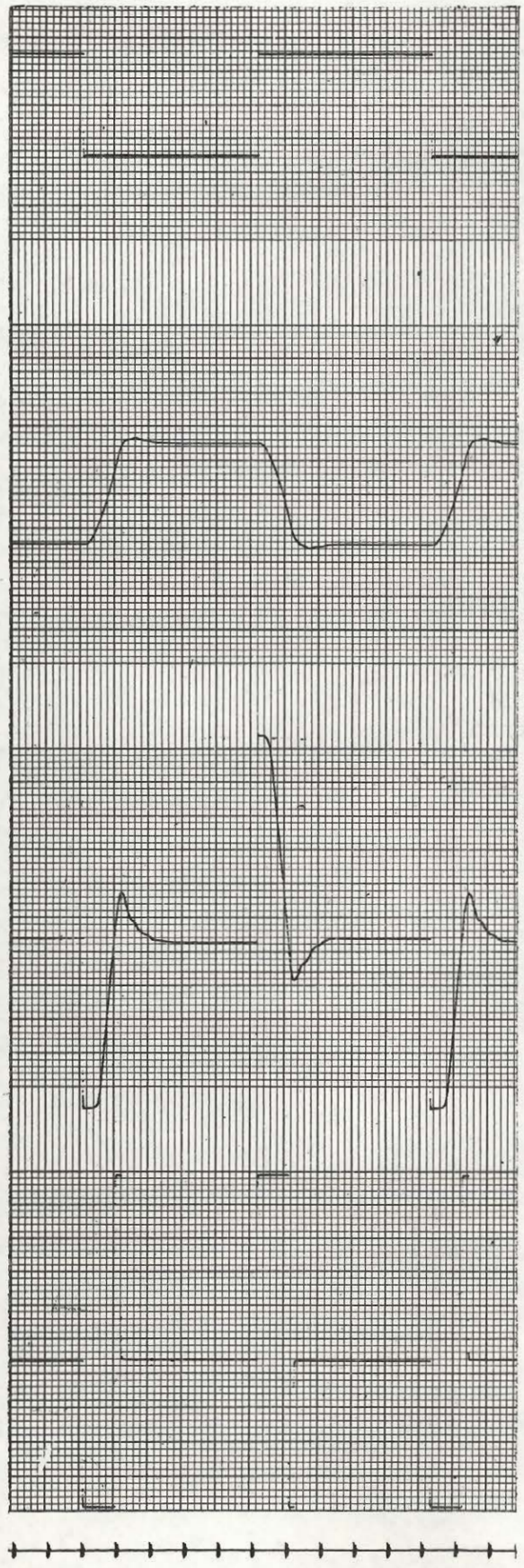

Fig. 4.1 Dual-Mode Linear Servo

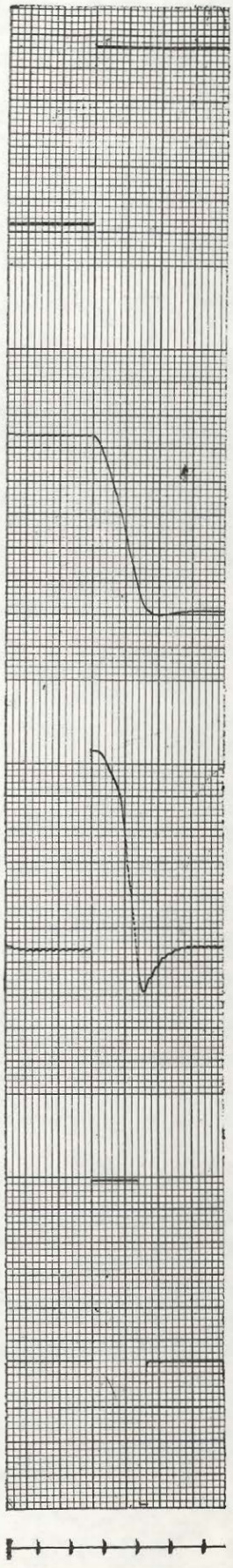

Fig. 4.1.1 Dual-Mode Carrier-Controlled Relay Servo

CARRIER-CONTROLLED RELAY SERVO

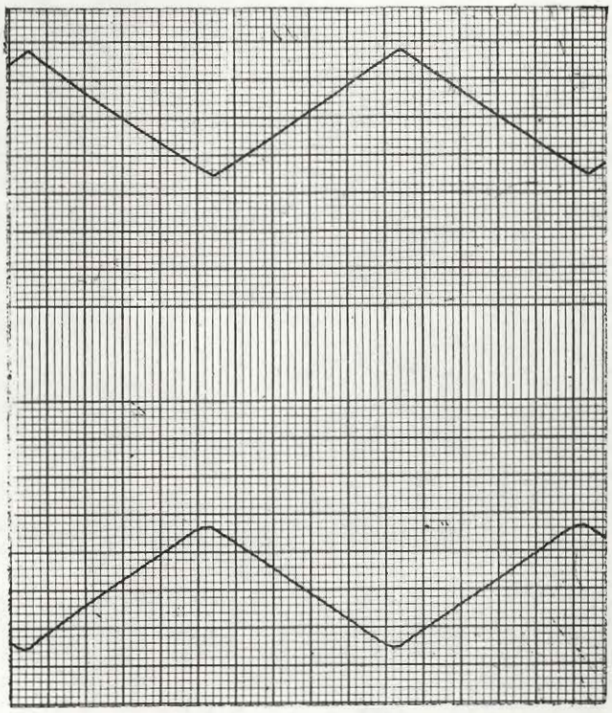

Fig. 4.2 Response to a Ramp-Input

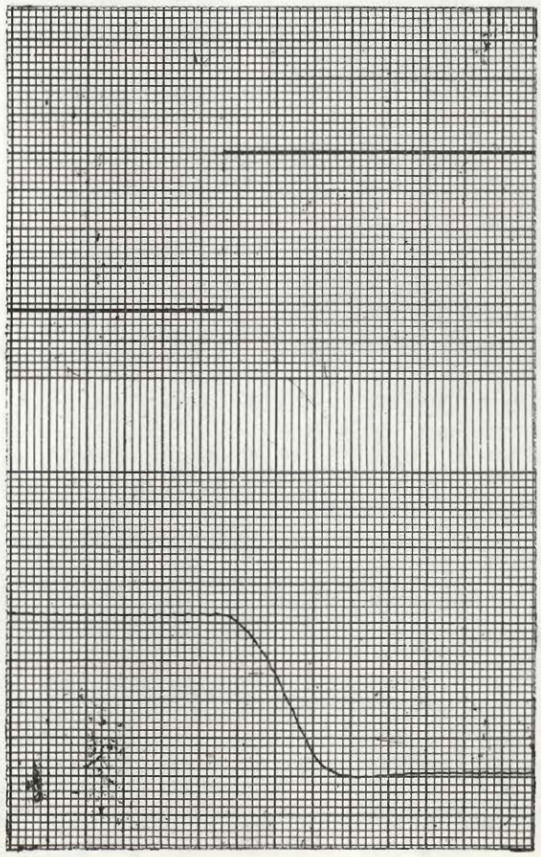

Fig. 4.3 Response to a Step-Input

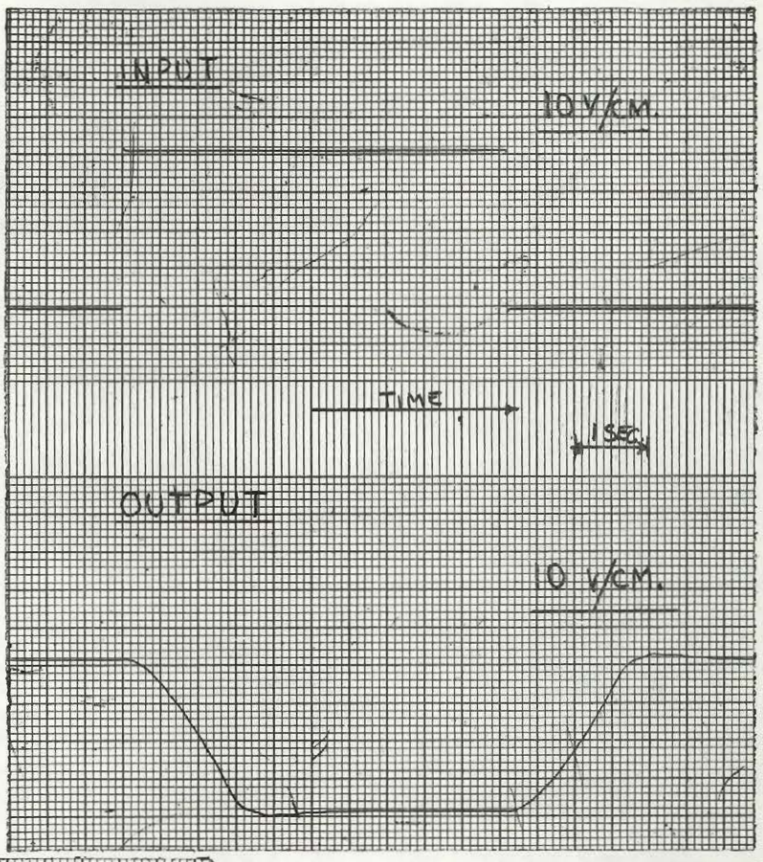

Fig. 4.4 Response of the Standard Linear Servo

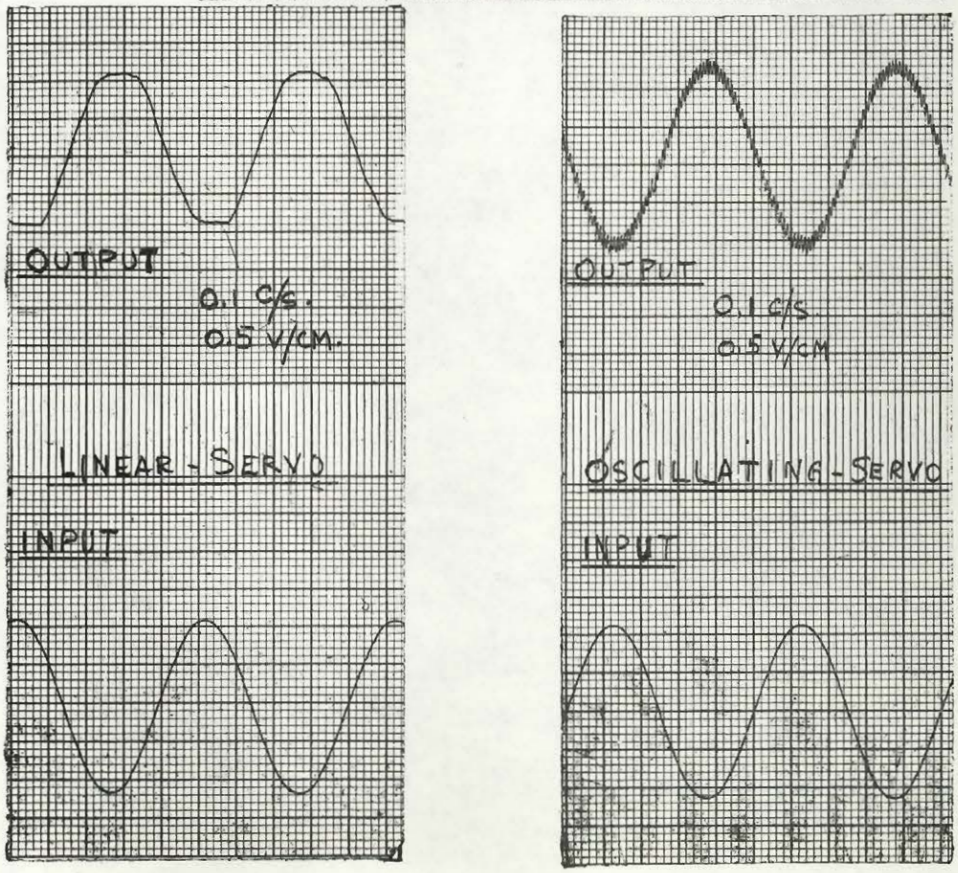

Fig. 4.5 Small Input Performance of the Linear and Oscillating Servos.

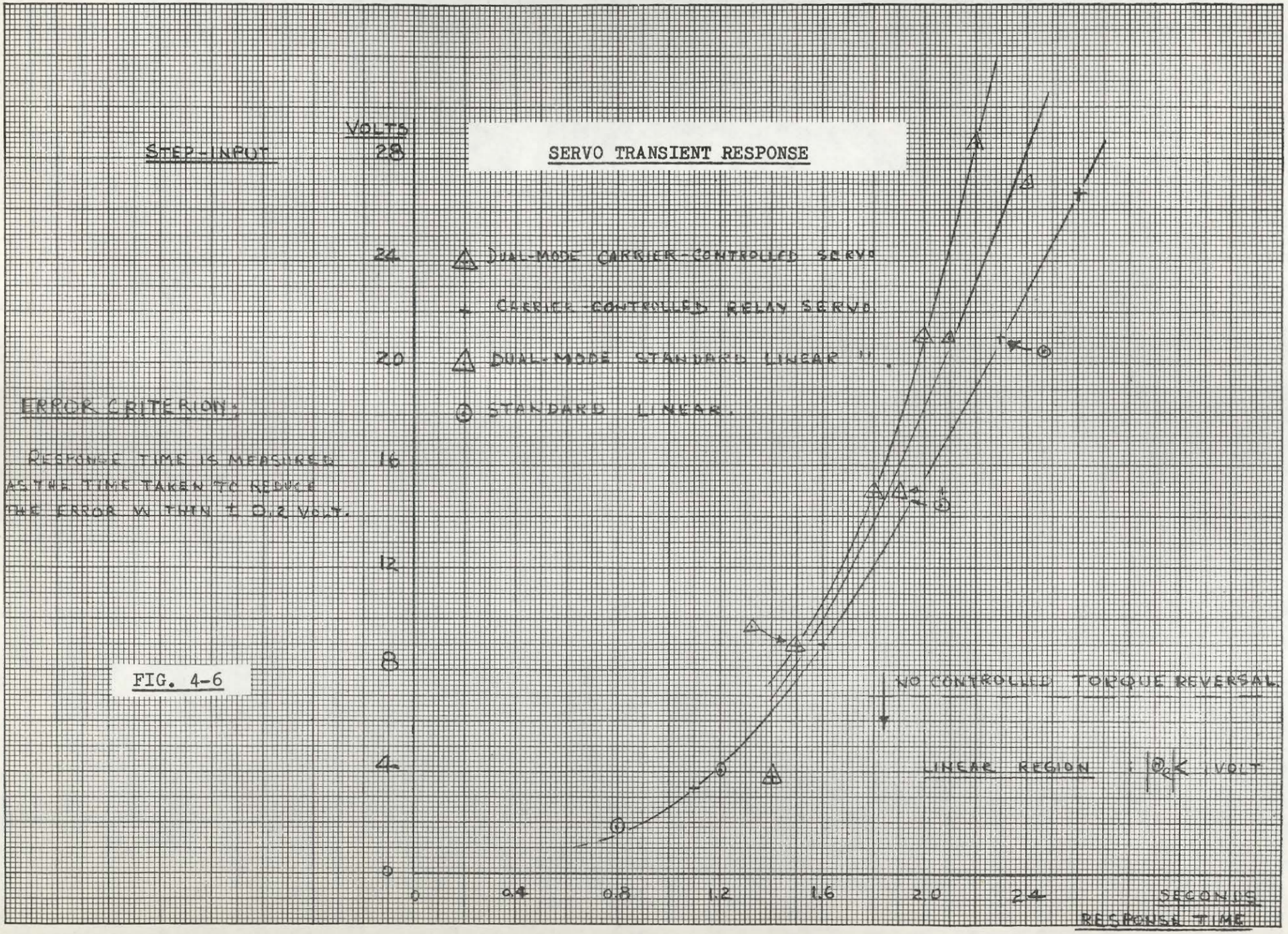

FIG. 4-6

allowing a ready comparison of the four types of servo control. The following conclusions were arrived at:

a. For inputs larger than 10 volts, the response time of all four systems increases approximately with the magnitude of the step.

b. In the vicinity of 10 volts, no significant differences could be detected in the speed of response.

c. Above 10 volts the curves start separating. The response of the dual-mode carrier-controlled servo is decidedly better than that of the others. At 26 volts, it is about 20% faster than both linear and carrier controlled servos and about 10% faster than the dual-mode linear.

d. There is no significant difference between the carrier-controlled and the "linear" servos as far as the response time is concerned. However, for low inputs the output of the linear servo had a tendency to be oscillatory in the final portion of the transient. This is probably due to backlash in the gears.

e. For small inputs the response of the dual-mode systems tends to be worse than that of the other two because the system enters the linear region before any torque reversal takes place.

f. For the carrier-controlled and the linear systems, the amount of overshoot reaches a maximum for inputs above a certain level and decreases for signals below that level.

g. For the dual-mode carrier-controlled system, the larger the input, the smaller the overshoot.

h. For the dual-mode linear servo, the amount of overshoot does not seem to have any definite relation to the input. This is probably due to the fact that the transition between the two modes initiates a transient at the output of the power amplifier.

4.2.2 Phase-plane diagrams.

The phase-plane diagrams help in understanding the above results by giving more insight into the operation of the different systems. The output (A) of the switching circuit is shown in some of them making evident the points of torque reversal and the region of linear control. Upon examining the phase-plane portraits, the following observations can be made.

a. The deceleration trajectory is very steep, indicating a high damping factor (F) in the motor and load combination.

b. The third-order nature of the system is evidenced by the rounded corner at the point of torque reversal and by the finite initial slope of the trajectories. This slope is equal to $\frac{1}{T_2} - \frac{1}{T_1}$.

c. Torque reversal does not take place for inputs below 7 volts.

d. All systems reach velocity saturation for any input larger than 22 volts. The torque reversal takes place at the same point for all these inputs.

e. The useful portion of the switching function is very short and could be approximated by a straight line of the form $(\theta_e + K\dot{\theta}_e + C) = 0$.

f. On diagrams (D) and (F) it can be seen that the point of torque reversal has to be advanced roughly 50 milliseconds ($T_2 \approx 50$ msec.).

g. Diagram (A) shows that the transition between modes is somewhat less accurate for the dual-mode "linear" system than for the dual-mode carrier-controlled system (B).

h. Diagram (C) reveals that the only difference between the servo operated as an on-off system with dead-zone and as a dual-mode system is the instability about the origin.

i. For the inputs causing velocity saturation, the carrier controlled servo (G) has a common deceleration trajectory which is a little steeper than in the dual-mode carrier-controlled case (D). The same is true for the systems using the linear controller, (E) and (F).

j. It has been noticed that reducing the linear region beyond a certain limit increased the overshoot in both dual-mode systems. This is due to the fact that the linear region must be wide enough to absorb the energy stored in the second time constant. In an optimum third-order system, this is done by a second application of positive torque, with a duration of the order of magnitude of (T_2).

4.3 Conclusions.

The dual-mode carrier-controlled servo is slightly better than the dual-mode standard for large enough inputs. An examination of the phase-plane in the linear mode reveals that in the standard system, a small transient is initiated after the switching of modes. This is probably due to the sudden change of the load of the power amplifier. The carrier-controlled dual-mode servo has the advantage that the switching is smoother and that the power is fed directly from the line. These advantages would be especially important in systems handling large loads.

The reasons why the on-off servos proved to have a speed of response of only 10% to 20% better than the other two are that:-

a. The dual-mode control was not exploited at its full potentiality due to very unfavorable conditions: high friction damping and velocity saturation.

b. The "linear" and the oscillating systems were operating at maximum capacity. Because they saturate at very low levels of input signals, they can be considered as on-off systems where the switching function is a linear combination $(\theta_e + K\dot{\theta}_e)$ of error and error-rate. Their only difference from the true dual-mode system is that the torque reversal takes place a little later.

The advantages of dual-mode control can be fully realized only for heavy systems where the ratio F/J is small. Since switching of high power is involved, the dual-mode carrier-controlled system will have a definite superiority over the standard type for the reason given above. This will eliminate the use of the amplidyne or the Ward-Leonard system. In very heavy systems like the one described in reference 28, the motor is kept running all the time and the switching takes place at the load by means of a clutch and a double gear system. One obvious advantage of this arrangement is in the reduction of the duty factor imposed on the motor which is constantly being started in a relay system.

The carrier-controlled and the linear servos have almost identical transient performance. The tracking accuracy is equally good in both systems. The superiority of the oscillating servo is apparent only when static accuracies are compared. The response of the linear servo is degraded for small inputs by the presence of backlash, static friction, etc. As shown in Figure 4.5, the accuracy of the oscillating

servo is excellent for a 0.1 c/s sinusoidal input of 0.6 volt peak-to-peak amplitude. The self-oscillation has a frequency of 5.0 c/s and an amplitude of 0.1 volt peak-to-peak. The output information can still be detected even for inputs of that order, because the output noise of the carrier-controlled servo is much less random than the output noise of the linear servo.

It must be noted that the conditions of their investigation were quite similar to those of an instrument servo, using a two-phase a.c. control motor with a high resistance, drag-cup rotor. The inertia is low and the friction factor high. Also, it saturates at small inputs and does not require much power. It is designed for accuracy and speed of response.

It can be concluded, then, that the carrier-controlled relay servo is ideally suited for the instrument servo. The dual-mode carrier-controlled relay servo will be used at its best in a heavy military or industrial system. This investigation has shown how the two methods of optimization and linearization can be applied together to obtain the best performance from a servo with inherent non-linearities. It has stressed the power of the superimposed carrier method as a means of linearization. This type of control has in addition a definite property of stabilization because the carrier signal produces a quenching of the non-linear oscillations that tend to take place. This idea has been used in process control. It is suggested that a thorough investigation of the stabilizing effect on a servomechanism should constitute a worthwhile project.

APPENDIX

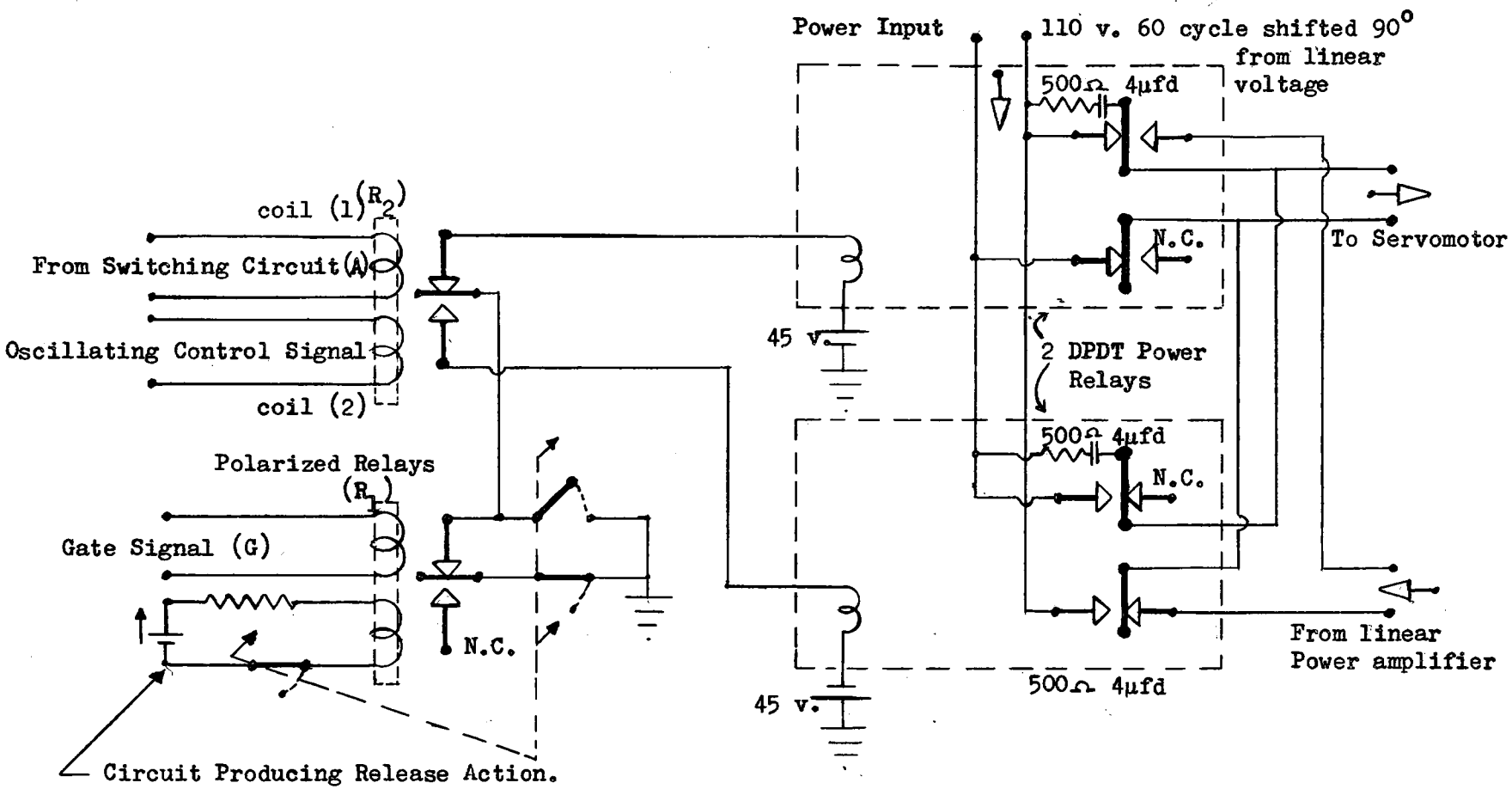

Actual Switch Position : Dual-Mode Standard
Other " " : Dual-Mode Carrier

N.C. : Not Connected

Relays

Polarized : N-E-280-E-G
Power : Potter and Brumfield
KCP-11

Fig. A-1 Relay Power Controller

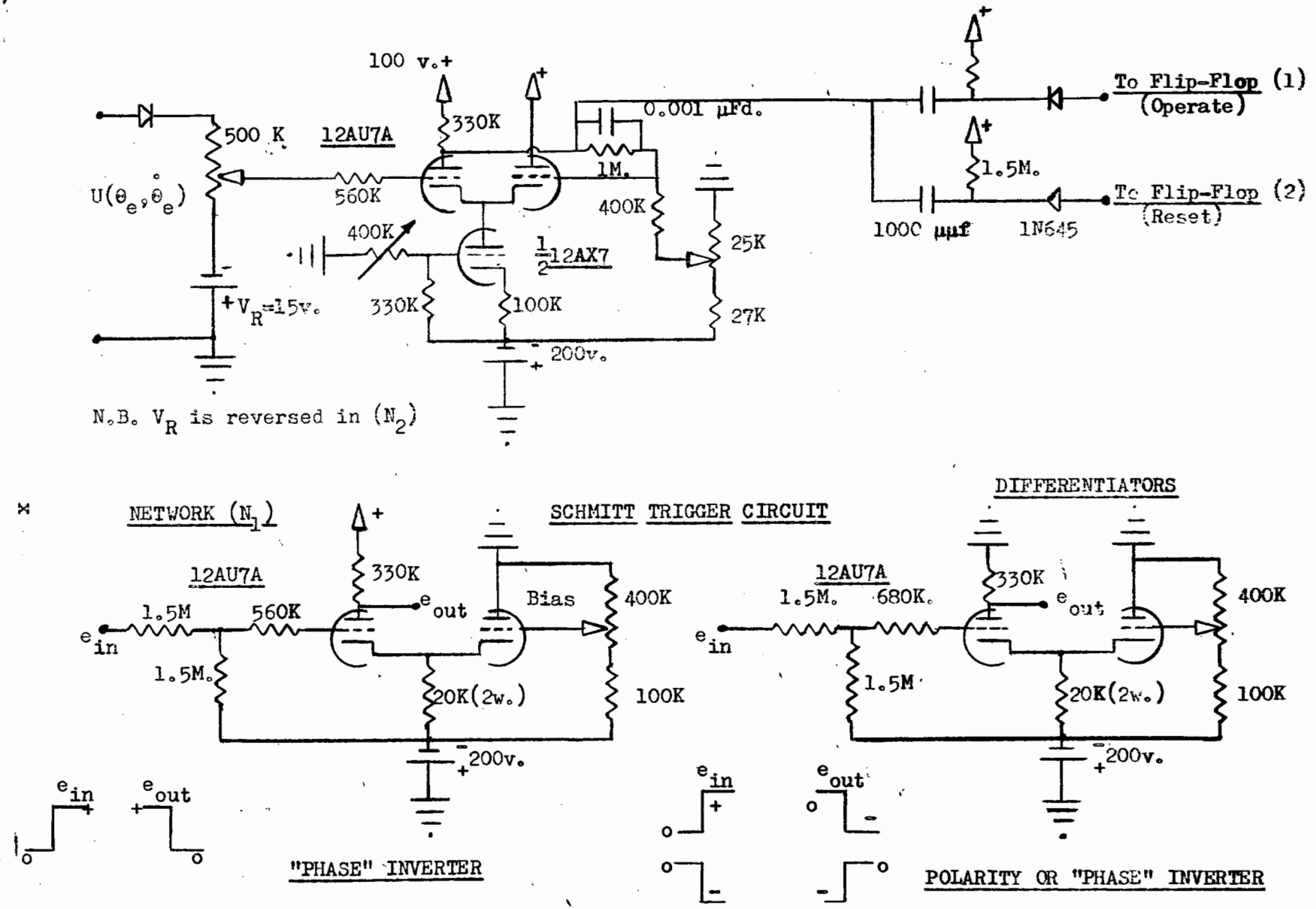

Fig. A-2.1 Electronic Switching Circuit (Components)

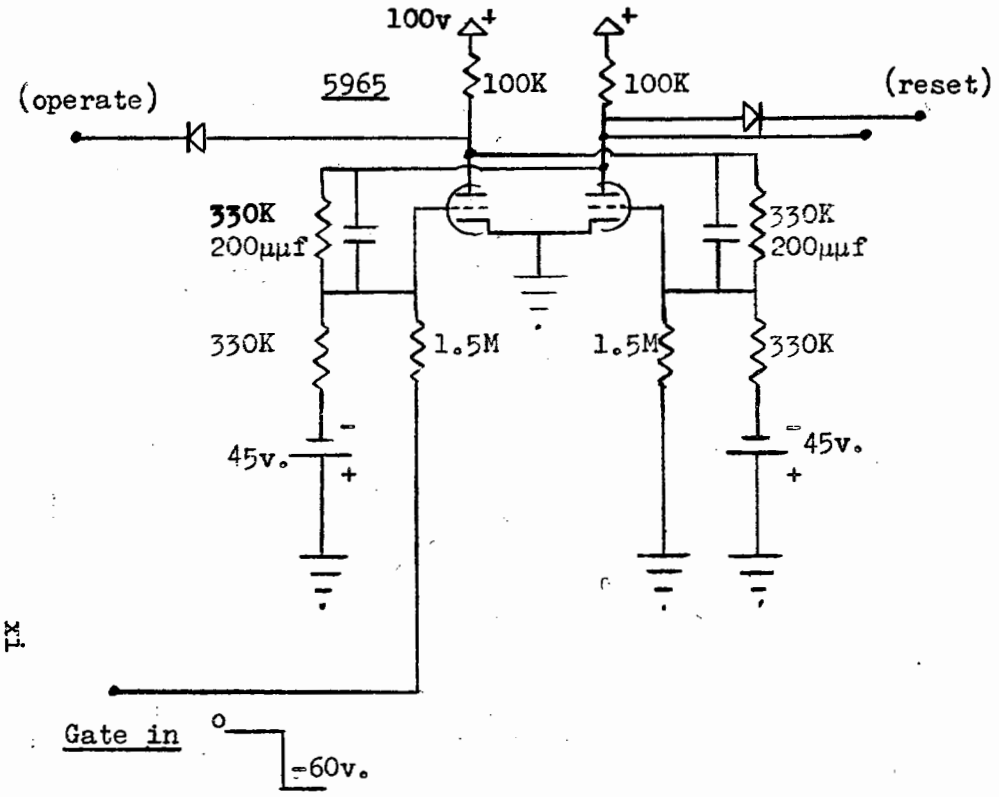

FLIP-FLOP

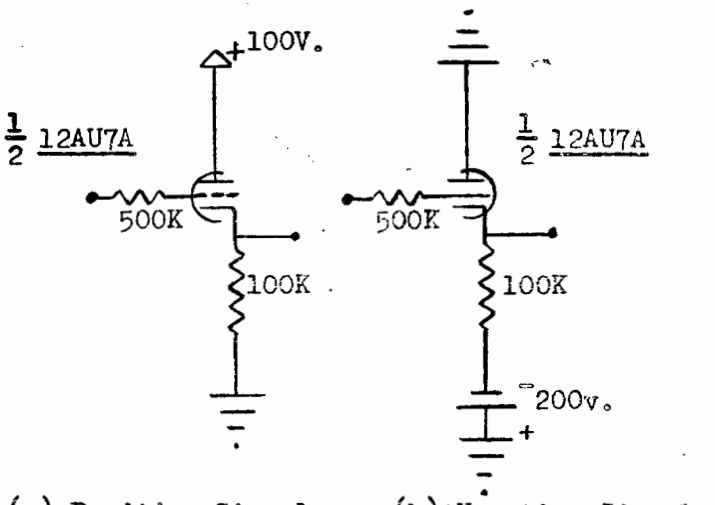

(a) Positive Signals (b) Negative Signals

CATHODE FOLLOWERS

N.B. POWER SUPPLIES

1) +100 v. (Red)

2) -200 v. (Blue)

Fig. A-2.2 Electronic Switching Circuit (Components).

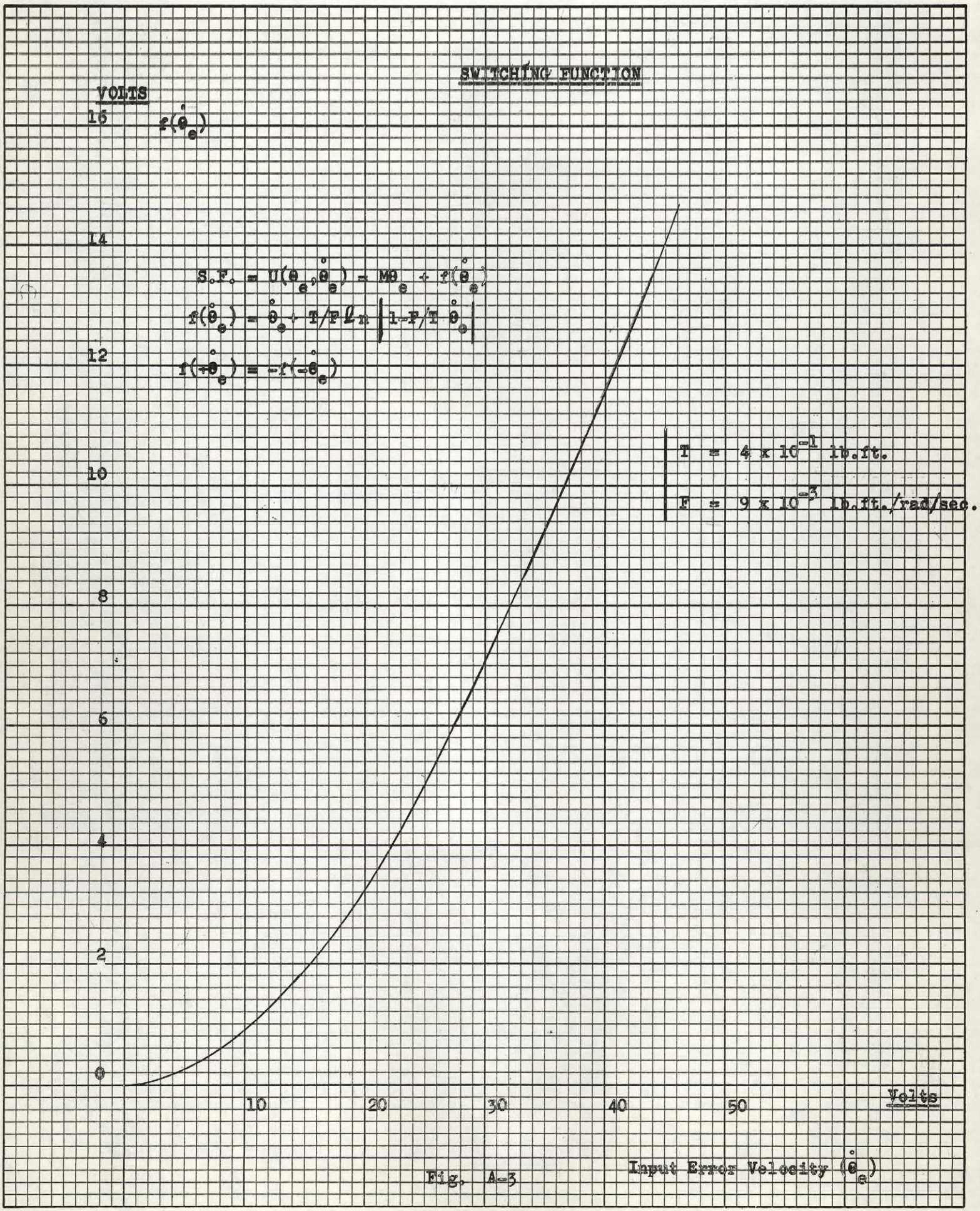
SWITCHING FUNCTION
VOLTS
15
$f(\dot{\theta}_e)$
14
$S.F. = U(\theta_e, \dot{\theta}_e) = M\theta_e + f(\dot{\theta}_e)$
$f(\dot{\theta}_e) = \dot{\theta}_e + T/F \ell_n \left| 1 - F/T\ \dot{\theta}_e \right|$
12
$f(+\dot{\theta}_e) = -f(-\dot{\theta}_e)$
$T = 4 \times 10^{-1}$ lb.ft.
$F = 9 \times 10^{-3}$ lb.ft./rad/sec.
10
8
6
4
2
0
10
20
30
40
50
Volts
Input Error Velocity ($\dot{\theta}_e$)

Fig. A-3

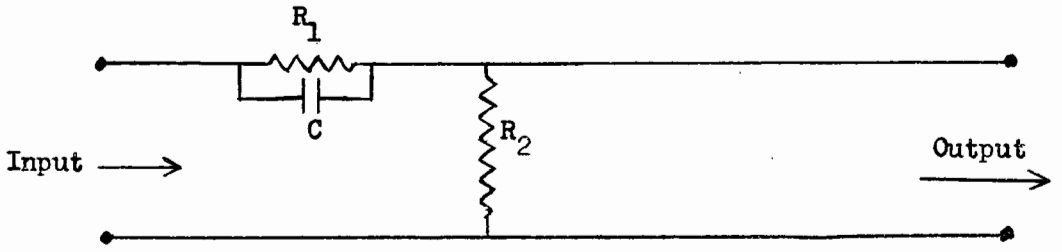

$$T(P) = \frac{R_2}{R_1+R_2} \frac{(1+PR_1C)}{\left(1 + P\frac{R_1R_2}{R_1+R_2}C\right)}$$

R_1 = 1.5 Mohm
R_2 = 150 Kohm
C = 0.2 μF

Design Data

Lead Phase Shift = $+\frac{\pi}{4}$

Frequency = 0.5 c/s

$$\frac{\omega R_1 R_2 C}{R_1+R_2} \gg 1$$

$$\omega R_1 C = 1$$

Fig. A-4 Phase Lead Network in Velocity Feedback Loop

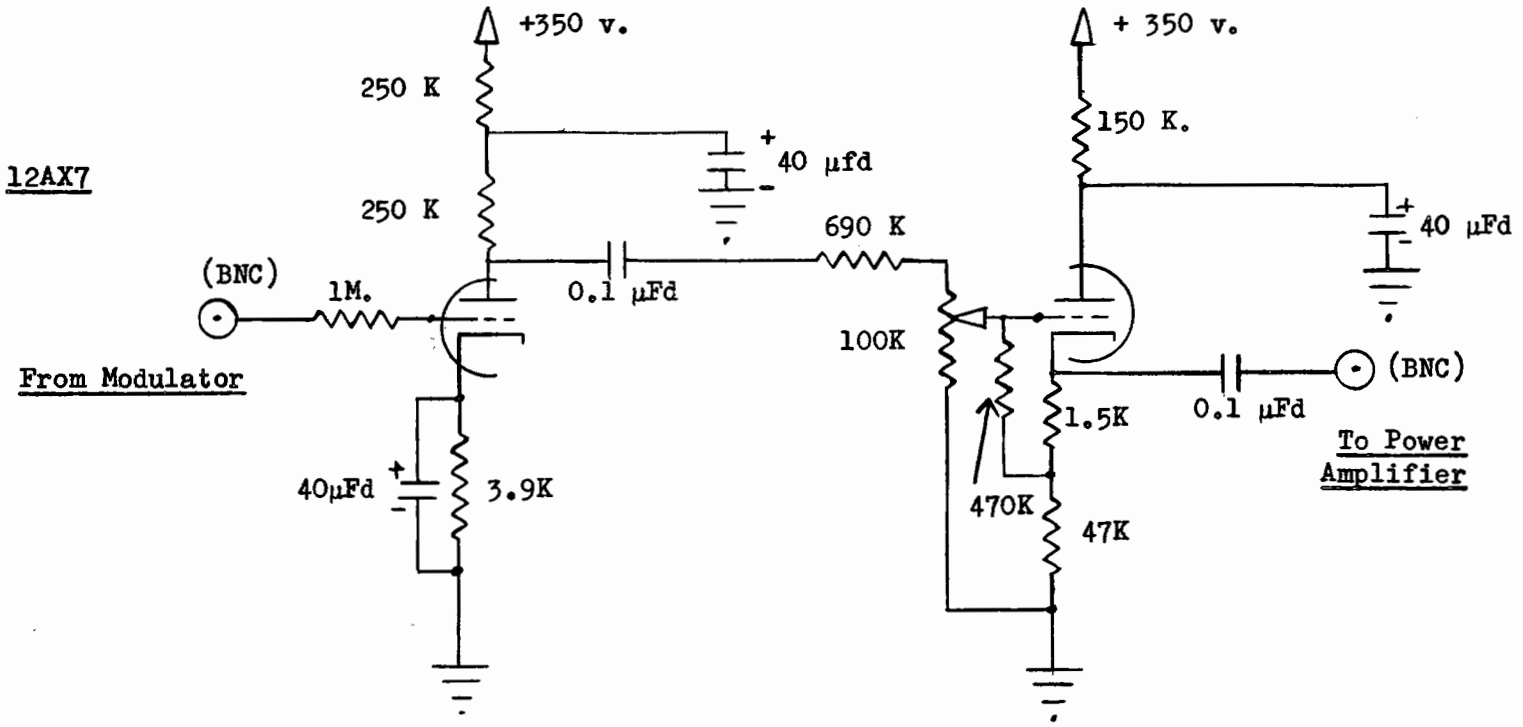

Max. Gain : 7.2

Fig. A-5 Modified Preamplifier

BIBLIOGRAPHY

1. Minorsky, N., "Directional Stability of Automatically Steered Bodies", Journal of the American Society of Naval Engineers, Vol. 34, 1922, pp. 280-309.

2. Hazen, A. L., "Theory of Servomechanisms", Journal of the Franklin Institute, Vol. 218, No. 3, September 1934, pp. 279-331.

3. Ferrel, E. B., "The Servo Problem as a Transmission Problem", Proceedings, I.R.E., Vol. 33, October 1945, pp. 763-767.

4. Bode, H. W., Network Analysis and Feedback Amplifier Design, D. Van Nostrand Company, 1945.

5. Nyquist, H., "Regeneration Theory," Bell System Technical Journal, Vol. 11, 1932, pp. 126-147.

6. Axelby, G. S., "Control Concepts", I.R.E. Transactions on Automatic Control, Vol. AC-4, May 1959, p. 1.

7. Tsien, H. S., Engineering Cybernetics, McGraw-Hill, 1954.

8. Higgins, T. J., "A Résumé of the Development and Literature on Non-Linear Control System Theory", A.S.M.E. Transactions, Vol. 79, 1957, p. 445.

9. Cosgriff, R. L., Non-Linear Control Systems, McGraw-Hill, 1959.

10. Smith, O. J. M., Feedback Control Systems, McGraw-Hill, 1958.

11. Gile, J. C., Pelegrin, M. J. and Decaulne, P., Théorie et Technique des Asservissements, Dounod (Paris), 1958.

12. Smith, O. J. M., "Availability of Necessary Theory for the Analysis and Design of Non-Linear Systems", I.R.E. Transactions on Automatic Control, PGAC-5, July 1958, pp. 60-61.

13. Bogner, I. and Kazda, L. F., "An Investigation of the Switching Criteria for Higher-Order Contactor Servomechanisms", A.I.E.E. Transactions, Vol. 73, Pt. II, July 1954, pp. 118-127.

14. Kochenburger, R. J., "A Frequency Response Method for Analyzing and Synthesizing Contractor Servomechanisms", A.I.E.E. Transactions, Vol. 79, Pt. I, 1950, pp. 220-284.

15. McDonald, D. C., "Non-Linear Techniques for Improving Servo Performance", Proceedings of the National Electronics Conference, 1950, p. 400.

16. Lewis, J. B., "Use of Non-Linear Feedback to Improve the Transient Response of a Servomechanism", A.I.E.E. Transactions, Vol. 71, Pt. II, January 1953, pp. 449-453.

17. Kuba, R. and Kazda, L., "A Phase-Space Method for the Synthesis of Non-Linear Servomechanisms", A.I.E.E. Transactions, Vol. 75, Pt. II, 1956, p. 282.

18. Kuba, R. and Kazda, L.F., "The Design and Performance of a Model Second-Order Non-Linear Servomechanism", I.R.E. Transactions, PGAC-5, July 1958, pp. 43-48.

19. Weiss, H. K., "Analysis of Relay Servomechanisms", Journal of Aeronautical Sciences (W.Y.), Vol. 13, July 1946, p. 364.

20. Dutilh, J. R., "Théorie des Servomécanismes a Relais", Onde Électrique, Vol. 30, October 1950, pp. 438-445.

21. MacColl, L. A., Fundamental Theory of Servomechanisms, Chapter 9, D. Van Nostrand Company, (New York), 1945.

22. Lozier, J. C., "Carrier-Controlled Relay Servos", Electrical Engineering, Vol. 69, December 1950, pp. 1052-1056.

23. Loeb, J. M., "De la Méchanique Linéaire a la Mechanique Non-Linéaire", Annales de Télécommunications, Vol. V, No. 2, February 1950.

24. Loeb, J. M., "A General Linearizing Process for Non-Linear Control Systems", Symposium on Automatic and Manual Control, Edited by A. Tustin, 1951, Cranfield, England.

25. Bellman, R., Glicksberg, I. and Gros, O., "On the 'Bank-Bang' Control Problem", Quarterly of Applied Mathematics, Vol. XIV, April 1956.

26. Silva, L. M., "Predictor Servomechanisms", I.R.E. Transactions, Vol. CT-1, No. 1, March 1954, p. 56.

27. Silva, L. M., "Predictor Control Optimalizes Control System Performance", A.S.M.E. Transactions, Vol. 77, 1955, p. 1317.

28. Kohlmeyer, K. W., "Clutch Servomechanisms, Design and Applications", Sperry Engineering Review, Vol. 12, No. 2, June 1959, pp. 10-19.

29. Caswell, C. F., "Investigation of the Response of Electromechanical Servomechanisms in Combined Linear and Non-Linear Operation", M.Eng. Thesis, McGill University, 1958.

30. Neiswander, R.S. and MacNeal, R.H., "Optimization of Non-Linear Control Systems by Means of Non-Linear Feedbacks", A.I.E.E. Transactions, Vol. 72, Pt. II, September 1953, p. 262.

31. Kalb, R. M. and Bennet, N. R., "Ferromagnetic Distortion of a Two-Frequency Wave", Bell System Technical Journal, Vol. 14, pp. 322-359.

32. Minorsky, N., "On Asynchronous Action", Journal of the Franklin Institute, Vol. 259, No. 3, 1955, pp. 209-219.

33. Oldenburger, R., "Signal Stabilization of a Control System", A.S.M.E. Transactions, Vol. 79, 1957, p. 1869.